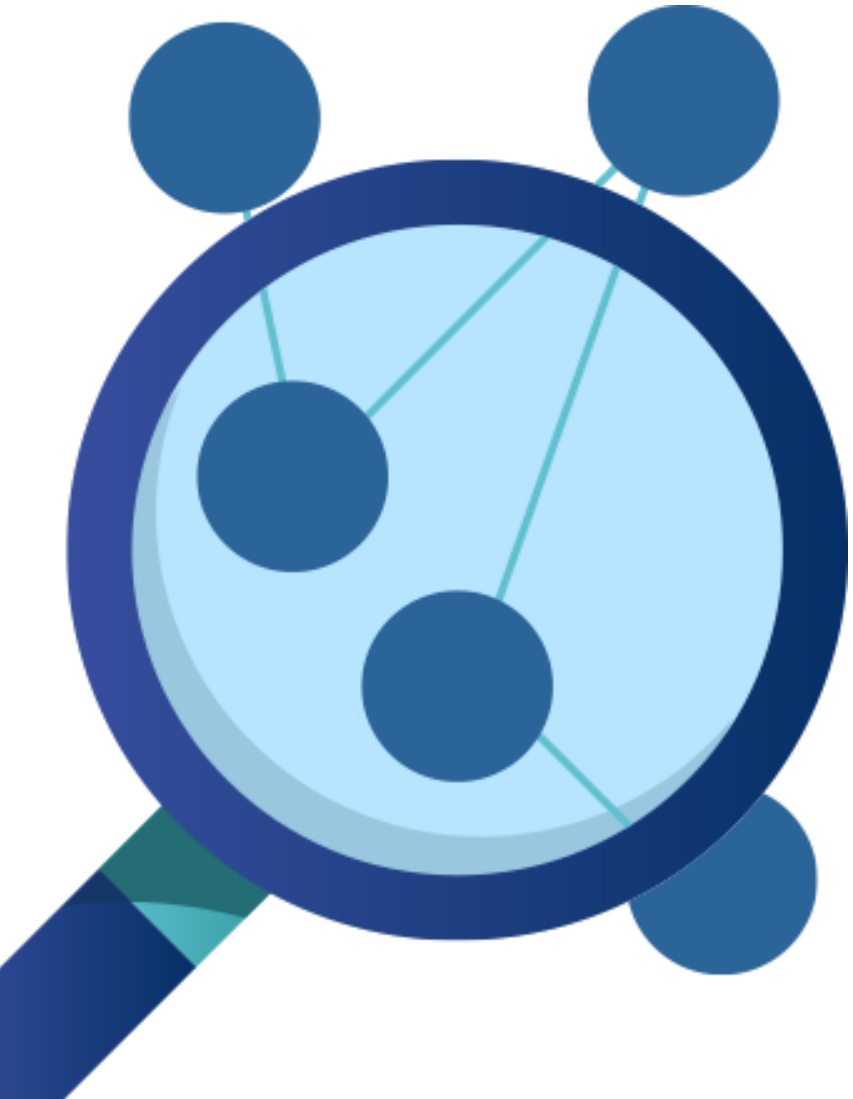
Prototype fluorescence tool

Deliverable D2.3

WP 2 SENSORS – Innovative monitoring systems



Author: Paolo Roccaro

Date: 31/05/2024

Funded by
the European Union

GRANT AGREEMENT NUMBER	101081728		
FULL TITLE / ACRONYM	INNOVATIVE TOOLS TO CONTROL ORGANIC MATTER AND DISINFECTION BYPRODUCTS IN DRINKING WATER - intoDBP		
START DATE	01/12/2022	**DURATION**	48 months
END DATE	30/11/2026		
PROJECT URL	**https://intodbp.eu/**		
DELIVERABLE	**2.3**		
WORK PACKAGE	**2**		
CONTRACTUAL DATE OF DELIVERY	**31.05.2024**		
ACTUAL DATE OF DELIVERY	**31.05.2024**		
NATURE	**DEM — Demonstrator, pilot, prototype**	**DISSEMINATION LEVEL**	SEN
LEAD BENEFICIARY	**UNICT**		
RESPONSIBLE AUTHOR	Paolo Roccaro		
CONTRIBUTIONS FROM	ATL, CANAL, ICRA, UCY		
ABSTRACT	This deliverable shows the development of a fluorescence-based tool and its adaptation for real-time measurement. This tool has been developed based on research carried out by the UCT team on the relationships between fluorescence indicators and the concentration of DBPs or DBPs precursors. In particular, the excitation/emission pairs, which were correlated to DBPs and/or DBPs precursors were employed in the customised fluorescence sensor. Laboratory and field experiments have been performed to compare the fluorescence signals obtained from the sensor and the laboratory spectrofluorometer. Data from intoDBP Case Studies (CSs) have been used to validate the tool in the laboratory. This task developed a customized fluorescence sensor as a tool to predict and monitor DBPs and DBPs precursors in disinfected waters that will be used online in the WP3 and WP4 actions.		

Disclaimer

Any dissemination of results reflects only the author's view and the European Commission is not responsible for any use that may be made of the information it contains.

Copyright message

© intoDBP Consortium, 2022
This deliverable contains original unpublished work except where clearly indicated otherwise. Acknowledgement of previously published material and of the work of others has been made through appropriate citation, quotation, or both. Reproduction is authorised provided the source is acknowledged.

TABLE OF CONTENTS

EXECUTIVE SUMMARY 5
LIST OF TABLES 6
LIST OF FIGURES 6
ABBREVIATIONS 8
1.0 INTRODUCTION 9
2.0 ABSORBANCE AND FLUORESCENCE MEASUREMENTS FOR PREDICTING DBPS FORMATION: A LITERATURE REVIEW 10
2.1 Absorbance of NOM and DBPs formation 10
2.1.1 Absorbance as a measurement of the reactivity of NOM to form DBPs 10
2.1.2 Absorbance as a measurement of changes in NOM chromophores related to DBPs formation during chlor(am)ination 11
2.2 Fluorescence of NOM and DBPs formation 12
2.2.1 2D fluorescence and association with DBPs 12
2.2.1 Fluorescence excitation emission matrix (EEM) (3D fluorescence) and its relation with DBPs formation 14
3.0 IDENTIFICATION OF FLUORESCENCE INDEXES SUITABLE FOR SENSOR DEVELOPMENT 18
3.1 EEM of water samples from Case Studies 18
3.2 Correlations between fluorescence indexes and DBPs 20
3.2.1 DBPs Formation Potential prediction 20
3.2.2 DBPs concentration monitoring 21
4.0 CORRELATIONS BETWEEN FLUORESCENCE MEASUREMENTS OBTAINED FROM SPECTROFLUOROMETER AND CUSTOMIZED SENSOR 23
4.1 Calibration of fluorescence sensors 23
4.2 Fluorescence sensors validation 25
4.2.1 Validation of fluorescence sensors with different water matrices 25
4.2.2 Validation of fluorescence sensors on samples from CS-1 (Limassol, Cyprus) 26

4.2.3 Validation of fluorescence sensors on samples from CS-2 (Barcelona, Spain) 30
4.2.4 Validation of fluorescence sensors on samples from CS-3 (Madrid, Spain) 32
4.2.5 Validation of fluorescence sensors using all data together from CSs 34

5.0 CORRELATIONS BETWEEN FLUORESCENCE SENSORS SIGNALS AND DBPS 35

5.1 DBP Formation Potential (DBPFP) 35
5.2 DBPs concentrations 40
5.2.1 Correlation between DBPs and fluorescence signals from all the distribution system points at CS-1 40
5.2.2 Correlation between DBPs and fluorescence signals from the sensor stations within the distribution system at CS-1 43

6.0 FLUORESCENCE TOOL CHARACTERISTICS 46

7.0 CONCLUSIONS 48

8.0 REFERENCES 50

EXECUTIVE SUMMARY

This deliverable shows the development of a fluorescence-based tool and its adaptation for real-time measurement. This tool has been developed based on research carried out by the UCT team on the relationships between fluorescence indicators and the concentration of DBPs or DBPs precursors. In particular, the excitation/emission pairs, which were correlated to DBPs and/or DBPs precursors were employed in the customised fluorescence sensor. Laboratory and field experiments have been performed to compare the fluorescence signals obtained from the sensor and the laboratory spectrofluorometer. Data from intoDBP Case Studies (CSs) have been used to validate the tool in the laboratory. This task developed a customized fluorescence sensor as a tool to predict and monitor DBPs and DBPs precursors in disinfected waters that will be used online in the WP3 and WP4 actions.

LIST OF TABLES

Table 1 Summary of absorbance-based surrogate water parameters used to monitor NOM reactivity in drinking water 12
Table 2 Summary of 2D fluorescence-based surrogate water parameters used to monitor DBPs and their precursor in chlorinated waters 14
Table 3 Summary of 3D fluorescence-based surrogates used to monitor NOM reactivity and DBPs formation in drinking water 16
Table 4. Excitation/emission pair of fluorescence sensors investigated in this project . 23
Table 5. Determination coefficients (R^2) of linear correlation models between fluorescence by sensors and actual DBPs detected in non-quenched Cyprus water samples collected from all the distribution points (February and March sampling campaigns) 41
Table 6. Determination coefficients (R^2) of linear correlation models between fluorescence by sensors and actual DBPs detected in quenched Cyprus water samples collected from all the distribution points (February and March sampling campaigns) .. 42
Table 7. R^2 coefficients of linear correlation models between fluorescence by sensors and actual DBPs detected in non-quenched Cyprus water samples collected at the sensor stations (February and March sampling campaigns) 44
Table 8. R2 coefficients of linear correlation models between fluorescence by sensors and actual DBPs detected in quenched Cyprus water samples collected at the sensor stations (February and March sampling campaigns) 44

LIST OF FIGURES

Figure 1. EEM of CS-1 (Limassol) samples collected at different points: a) Raw water, b) Post Aeration, c) Post Sand Filter, d) Final treated, e) Outlet, f) Inlet, g) Distribution 1, h) Distribution 2 18
Figure 2. EEM of CS-3 (Madrid) samples collected at different points: a) raw water, b) Pre Ozone, c) Post Filter, d) Post Activated Carbon, e) Outlet, f) Distribution 1, g) Distribution 2, h) Distribution 3 19
Figure 3. EEM of CS-2 (Barcelona) samples collected at different points: a) raw water, b) Post clarified, c) Post AC, d) Outlet, e) Distribution 1, f) Distribution 2, g) Distribution 3 19
Figure 4. Correlation between ΔI3 or ΔI5 and DBPFP in chlorinated ATL (CS-2) waters (raw, clarified, GAC filtered, outlet) in two different sampling days 20
Figure 5. Correlation between I3 or I5 and DBPFP in chlorinated ATL (CS-2) waters (raw, clarified, GAC filtered, outlet) in two different sampling days 21
Figure 6. Correlation between I3 and DBPFP in chlorinated Madrid (CS-3) waters (raw, pre-ozonated, sand filtered, GAC filtered, outlet) in two different sampling days 22
Figure 7. Calibration lines of the five fluorescence sensors on Limassol (a) and Canal (b) raw waters 24
Figure 8. Linear correlation between fluorescence indexes measured by sensors and lab-scale spectrofluorometers of four diluted samples of two different surface waters 25

Figure 9. Linear relationship between fluorescence measurements by sensors and lab-spectrofluorometer for a set of different water matrices 26
Figure 10. Location of sampling point for the CS1 (Cyprus) case study 27
Figure 11. Fluorescence EEMs of non-quenched samples from the Cyprus case study (February sampling campaign) 28
Figure 12. Fluorescence EEMs of quenched samples from the Cyprus case study (February sampling campaign) 28
Figure 13. Fluorescence intensities obtained with I3 and I5 sensors from quenched and not-quenched samples from CS-1 29
Figure 14. Linear correlation between the values of fluorescence intensity I3 or I5 obtained by the spectrofluorometer (Arbitrary Units) and the fluorescence signals from sensors I3 or I5 for CS-1 29
Figure 15. Simplified scheme of the DWTP managed by ATL (Barcelona case study) 30
Figure 16. Reduction of fluorescence peaks (I3 and I5) by sensors during treatment stages and distribution system of water samples from CS-2 31
Figure 17. Linear correlation between the values of fluorescence intensity I3 or I5 obtained by the spectrofluorometer (Arbitrary Units) and the fluorescence signals from sensors I3 or I5 for CS-2 32
Figure 18. Simplified scheme of the DWTP managed by Canal (Madrid case study) .. 32
Figure 19. Reduction of fluorescence peaks (I3 and I5) by sensors during treatment stages and distribution system of water samples from CS-3 33
Figure 20. Linear correlation between the values of fluorescence intensity I3 or I5 obtained by the spectrofluorometer (Arbitrary Units) and the fluorescence signals from sensors I3 or I5 for CS-3 33
Figure 21. Linear correlation between the values of fluorescence intensity I3 or I5 obtained by the spectrofluorometer (Arbitrary Units) and the fluorescence signals from sensors I3 or I5 for all CSs data together (CS-1+CS-2+CS-3) 34
Figure 22. THMs concentration detected in Cyprus water samples from FP tests carried out on February (a) and March (b) sampling campaigns 36
Figure 23. Linear correlations between fluorescence sensors I3 or I5 and trihalomethanes in FP tests performed in Cyprus water samples (March sampling campaign) 38
Figure 24. Linear correlations between differential fluorescence by sensors ΔI3 or ΔI5 and trihalomethanes in FP tests performed in Cyprus water samples (March sampling campaign) 40
Figure 25. THMs levels in Cyprus samples (average values of February and March campaigns) 41
Figure 26. Linear correlations between actual DBPs concentrations and fluorescence signals sensor I5 detected in CS-1 quenched and non-quenched samples collected from all the points of the distribution system points (February sampling campaign) 43
Figure 27. Linear correlations between actual DBPs concentrations and fluorescence by sensor I5 detected in Cyprus quenched and non-quenched samples collected at the sensor stations (February sampling campaign) 45
Figure 28. Picture of the Photometric Transmitter (PT) (top) and probe (bottom) of the customized fluorescence tool 46
Figure 29. Detail of an online connection of the fluorescence probe 47

ABBREVIATIONS

Abbreviation	Description
CS	Case Study
DBPs	Disinfection by-products
DOC	Dissolved Organic Carbon
DOM	Dissolved Organic Matter
DWTP	Drinking Water Treatment Plant
EEM	Fluorescence excitation-emission matrix
NOM	Natural Organic Matter
SUVA	Specific UV absorbance
THMs	Trihalomethanes
THMFP	Trihalomethanes Formation Potential
TTHMs	Total Trihalomethanes
UV	Ultraviolet

1.0 INTRODUCTION

This report is the deliverable D2.3 of task 2.2, work package 2. This deliverable shows the development of a fluorescence-based tool and its adaptation for real-time measurement.

The UCT team has developed the fluorescence-based tool using literature data (§2) and laboratory data (§3) that demonstrated strong relationships between selected fluorescence indexes and the concentration of DBPs or DBPs precursors. Furthermore, data from intoDBP Case Studies (CSs) has been used to validate the tool (§3). In particular, the excitation/emission pairs, which were correlated to DBPs and/or DBPs precursors were employed in the customised fluorescence sensor. Experiments have been performed to compare the fluorescence signals obtained from the sensor and the fluorescence data from the laboratory spectrofluorometer (§4). Finally, the fluorescence signals have been used to predict DBPFP in DWTPs and to track DBPs levels in the distribution systems of the CSs (§5).

The scope of this report is to develop and validate offline a prototype fluorescence tool designed to predict and monitor the formation of DBPs in waters collected from the intoDBP CSs. This activity has been carried out by the UCT team in task 2.2 of WP2. The activity has involved other partners. Indeed, ATL, CANAL, and UCY have provided the water samples from the CSs, ICRA has provided DBPs and fluorescence data from CS-3 used in §3, and UCY has provided the DBPs data from CS-1 used in §4 and 5. The developed prototype fluorescence tool will be employed online in the WP3 and WP4 actions.

2.0 Absorbance and fluorescence measurements for predicting DBPs formation: a literature review

2.1 Absorbance of NOM and DBPs formation

2.1.1 Absorbance as a measurement of the reactivity of NOM to form DBPs

Spectroscopic surrogates have been proposed to monitor a wide range of water quality parameters, including conventional parameters (e.g., COD, BOD_5), pathogens, disinfection by-products (DBPs) and trace organic contaminants (Korshin et al., 2018).

NOM absorption of both visible and UV light is widely attributed to the aromatic chromophores (light absorbing) present in NOM molecules (primarily humics) dissolved in the water. Absorbance of ultraviolet light at 254 nm (A254) and the specific value (SUVA254), which is the ratio between A254 and DOC, are the most widely used surrogate parameters to measure and characterize NOM (Croue et al., 2000; Karanfil et al., 2002; Kitis et al., 2002, 2001). The choice of such wavelength is because the absorbance at 254 nm is a measure of the overall content of activated aromatic groups in PHA moieties (Croue et al., 2000; Korshin et al., 1996; Traina et al., 1990). In particular, SUVA254 has been widely used because it allows the comparison of different water sources in terms of reactivity for DBPs formation, usually measured as THMs Formation Potential (THMFP) (APHA, 1998) or uniform formation condition protocol (UFC) (Summers et al., 1996).

Although $SUVA_{254}$ is the surrogate parameter used for predicting NOM reactivity, SUVA measurements can be influenced by the pH, nitrate, and iron and more generally questions are raised about the strength of SUVA as an indicator of DOC reactivity (Weishaar et al., 2003). Furthermore, the absorbance at 280 nm was also introduced because π-π* electron transition occurs in this UV region (ca. 270– 280 nm) for phenolic substances, aniline derivatives, benzoic acids, polyenes and polycyclic aromatic hydrocarbons with two or more rings (Traina et al., 1990).

Strong relationships between the molar absorbance of organic carbon at 280 nm (ε_{280}) and, on the other hand, the aromaticity of NOM and its apparent number- and weight-averaged molecular weight have been found (Chin et al., 1994; Croue et al., 2000; Peuravuori et al., 2005; Peuravuori and Pihlaja, 2004, 1997). Absorbance UV at both 254 and 272 nm were well correlated with aromaticity, which is the percentage of the total carbon contained in aromatic subgroups (Chin et al., 1994; Peuravuori and Pihlaja, 1997; Traina et al., 1990; Wu et al., 2000, p. 200).

Overall, UV_{254}, UV_{272} and UV_{280} absorbance are more sensitive surrogate parameters for predicting NOM reactivity in DBP formation than DOC. Finally, differential absorbance at wavelengths near 272 nm (ΔA_{272}), corresponding to the peak of differential absorbance, was also used because it showed a strong correlation with DBPs similar to $SUVA_{254}$ (Roccaro and Vagliasindi, 2009).

2.1.2 *Absorbance as a measurement of changes in NOM chromophores related to DBPs formation during chlor(am)ination*

Various methods have been developed for monitoring DBPs concentration by using UV-VIS spectroscopy. For instance, differential absorption spectroscopy (DAS), defined as the difference in UV absorbance spectra before and after chlorination (also referred as ΔA), has shown great potential to predict and monitor DBPs levels in chlor(am)inated waters. This method quantifies changes in the UV–visible absorbance of dissolved organic matter (DOM) caused by reactions of its chromophores with chlorine or chloramine.

Different wavelengths have been used to apply the DAS approach. ΔUV_{254}, ΔUV_{272} and ΔUV_{280} absorbance are the most used parameters to predict/monitor DBPs in chlor(am)inated waters. Furthermore, the differential absorbance at 350 nm ($-\Delta A_{350}$) with its logarithm were demonstrated useful to monitor the formation of DBPs. As a result of its precision and sensitivity, DAS serves as a powerful tool for characterizing the formation of DBPs generated during chlorination or chloramiantion of natural water. However, the use of DAS to estimate DBPs has been found seasonally specific (Beauchamp et al., 2018).

The nonlinear relationship between the intensity of DAS and DBP concentrations, as well as the need to develop site-specific fitting parameters, limits its practical applications (Deng et al., 2024). Furthermore, other problems may arise under different conditions. For example, the presence of chlorine, chloramines, and other chemicals impacts absorbance spectra. Furthermore, absorbance-based techniques can only determine the content of the aromatic functional groups in OM with no information provided on the presence and of non-chromophoric OM (Bridgeman et al., 2011).

Another difficulty in using absorbance-based techniques for water quality monitoring is that the absorbance spectra comprise contributions of multiple chromophores and inter-chromophores interactions, resulting in featureless spectra (Korshin et al., 2018). As a result, it is difficult to decompose and characterize DOM to correlate precursors and DBPs. Despite such limitations, UV-VIS spectrophotometry is widely used for monitoring water quality and DBPs formation. Table 1 summarizes absorbance-based surrogates used to monitor NOM reactivity in drinking water.

Table 1. Summary of absorbance-based surrogate water parameters used to monitor NOM reactivity in drinking water

Parameter	Description	Reference
A_λ	Standard UV absorbance parameter used to detect different substances present in water.	(Dejaeger et al., 2022; Korshin et al., 2018)
A_{254}/A_{202}	Ratio of absorbance at 254 and 202 nm; a measure of activation of NOM.	(Dejaeger et al., 2022; Korshin et al., 2018)
$\Delta A_\lambda/A_{\lambda,0}$	Relative treatment-induced change of water absorbance at wavelength λ.	(Korshin et al., 2018)
$\Delta A_\lambda = A_{\lambda,0} - A_{\lambda,treated}$	Differential change of water absorbance at wavelength l determined vs. the absorbance prior to treatment.	(Korshin et al., 2018; Roccaro et al., 2008; Zhang et al., 2021)
$ASI=0,56(A_{254} \times A_{272})/(A_{220} \times A_{230})$	Absorbance slope index; deemed to be a measure of the molecular weight of NOM and its activity.	(Korshin et al., 2018)
$SUVA_{254} = A_{254}/DOC$	Commonly used to compare different water sources in terms of their reactivity for DBP formation.	(Hua et al., 2020; Korshin et al., 2018)
ΔA_λ	Differential absorbance at different wavelength. Quantifies changes in the UV–Visible absorbance of dissolved organic matter (DOM) caused by reactions of its chromophores.	(Beauchamp et al., 2018; Deng et al., 2024; Roccaro and Vagliasindi, 2009)
ΔA_{350}	Differential absorbance at 350 nm. Indicative of the action of the cyclic enones-like functional groups to form DBPs.	(Deng et al., 2024)
Logarithm of ΔA_{272} and ΔA_{350}	Prediction of DBP formation, variation among different water sources due to differences in DOM heterogeneity	(Deng et al., 2024; Zhang et al., 2020)

2.2 Fluorescence of NOM and DBPs formation

2.2.1 2D fluorescence and association with DBPs

Fluorescence is defined as the luminescence of a substance following the absorption of electromagnetic radiation. Luminescence is a process in which an atom or molecule emits light radiation during a transition from a higher-energy electronic level to a lower one. The fluorescence spectroscopy involves generating an emission spectrum by scanning the emission wavelength (λ_{em}), while the sample is irradiated at a single excitation wavelength (λ_{ex}). Similarly, an excitation spectrum is obtained by scanning the excitation wavelength while recording the emission signal at a single wavelength. 2D fluorescence is a measurement of this luminescence at a fixed excitation wavelength. In this way we obtain a measure of the emission fluorescence peaks at a single wavelength excitation. 2-D fluorescence, in contrast to absorbance, allows the detection of a big

range of fluorophores, but the output is restricted to a linear scan, in which the choice of excitation wavelength determines the molecules that may be identified (Hudson et al., 2007). The 2D spectra allow to determine some index calculated as the ratio between the fluorescence intensity obtained at different emission wavelengths. For example, a fluorescence index (FI), which is the ratio of the emission intensity at 450 nm to 500 nm (I_{450}/I_{500}), obtained with an excitation of 370 nm, was developed to distinguish the sources of aquatic humic acids (microbially and terrestrially derived) and was correlated with the aromaticity of fulvic acids (McKnight et al., 2001). Other indexes, namely the biological index (BIX) and the humification index (HIX) have been proposed. The BIX is calculated as the ratio of fluorescence intensities with emission wavelengths of 380 and 430 nm (BIX = F380/F430) at an excitation wavelength of 245 nm. This index varies in a value range from 0 to > 1 and indicates if the biological sources are mainly influenced by organisms or human activities. The HIX is the ratio of the average light intensity in the range of 435–480 nm and 300–345 nm when the excitation wavelength is 245 nm and is an indicator for humification degree or humic character. The FI, BIX, and HIX have been used to distinguish the sources of DOM (microbial or terrestrial). The FI has also been used to evaluate the water quality indicators of COD, 5-day BOD, total nitrogen, and ammoniacal nitrogen. Moreover, it has been shown that the FI can be used to evaluate emerging contaminants, such as DBPs, and their potential for formation (Jing et al., 2022).

Some fluorescence indices have been developed to track the formation of disinfection by-products (DBPs). A notable correlation was found between DBP formation and shifts in the wavelength corresponding to 50% of the maximum fluorescence intensity ($\lambda_{0.5}$) recorded at 320 nm excitation (Fabbricino and Korshin, 2005). Furthermore, Roccaro et al. (2009) have found that the differential value of the index I_{500}/I_{450} ($\Delta I_{500}/I_{450}$) obtained at 320 nm excitation is strongly correlated with the concentration of DBPs at varying chlorination conditions (raw and treated water, chlorine dose, reaction time, and temperature). These claims support the conclusion that the changes in these fluorescence indexes are indicators of the degree and outcome of NOM halogenation.

Synchronous fluorescence spectroscopy (SFS) is based on synchronous scanning technology. This method has been used in the identification and quantitation of complex mixtures. In SFS, the excitation and emission wavelengths are scanned at the same time, and a spectrogram is constructed from the measured fluorescence intensity and excitation wavelength (emission wavelength). The main types of SFS are constant-wavelength SFS (CWSFS), in which the excitation wavelength and emission wavelength are kept at a constant interval during fluorescence scanning; the constant-energy SFS (CESFS), a method to keep a constant excitation energy and emission monochromator during wavelength scanning; the variable-angle SFS and the matrix isopotential SFS. SFS has been applied to the detection of organic substances such as polycyclic aromatic hydrocarbons (PAHs) and pesticides in water, the determination of humic and fulvic acids, and analysis of water toxicity. Although SFS has been widely used in various fields, its application is limited by the internal filtration effect, fluorescence quenching and Raman and Rayleigh scattering (Jing et al., 2022).

Table 2 summarizes the main 2D fluorescence-based surrogates used to monitor DBPs and their precursor in chlorinated waters.

Table 2. Summary of 2D fluorescence-based surrogate water parameters used to monitor DBPs and their precursor in chlorinated waters

Method / Index	Description	Application
Fluorescence Index I_{450}/I_{500}	Ratio of the emission intensity at 450 nm to 500 nm (I_{450}/I_{500}) with an excitation of 370 nm. Used to distinguish sources of aquatic humic acids.	(McKnight et al., 2001; Roccaro et al., 2009)
$\lambda_{0.5}$ Index	Shift in the wavelength corresponding to 50% of the maximum fluorescence intensity. Used in the correlation with disinfection by-products (DBP) formation.	(Fabbricino and Korshin, 2005)
$\Delta(I_{500}/I_{450})$ Index,	Change in the ratio of emission intensity at 500 nm to 450 nm. Indicative of contraction of NOM (Natural Organic Matter).	(Roccaro and Vagliasindi, 2009)
$\Delta\lambda_{0.5}$ Index	Change in the shift of the entire NOM emission band. Used to quantify the shift of NOM emission band.	(Roccaro and Vagliasindi, 2009)
Synchronous Fluorescence Spectroscopy (SFS)	Technique where excitation and emission wavelengths are scanned simultaneously, generating a spectrogram. Identification and quantitation of complex mixtures, detection of organic substances, wastewater analysis.	(Jing et al., 2022)
Constant-Wavelength SFS (CWSFS)	Method maintaining constant interval between excitation and emission wavelengths during fluorescence scanning. Detection of pollutants such as PAHs, pesticides, determination of humic and fulvic acids, water toxicity analysis.	(Jing et al., 2022)
Constant-Energy SFS (CESFS)	Technique ensuring constant excitation energy and emission monochromator during wavelength scanning. Analysis of organic substances, determination of water quality parameters.	(Jing et al., 2022)
Variable-Angle SFS	Method varying excitation and emission angles to enhance spectral resolution. Improved detection and characterization of organic substances in water.	(Jing et al., 2022)
Matrix Isopotential SFS	Technique maintaining constant potential across the sample matrix during wavelength scanning. Enhanced analysis of complex mixtures, identification of contaminants.	(Jing et al., 2022)

2.2.1 Fluorescence excitation emission matrix (EEM) (3D fluorescence) and its relation with DBPs formation

Fluorescence excitation-emission matrix (EEM) spectroscopy, also known as three-dimensional fluorescence (3DEEM) or fluorescence fingerprinting, is one of the most predominant methods because of its information-rich data, visual maps and multidimensional information provided (Li et al., 2020). Indeed, fluorescence is often measured through a range of excitation and emission wavelengths using Excitation-Emission Matrix Spectroscopy (EEMs), producing a 3-D fluorescence intensity landscape in which the presence of distinctive peaks can provide indications of sources, behaviour, and biogeochemical cycling of DOM (Murphy et al., 2010), responsible for DBPs formation. The analysis of 3-D fluorescence data containing additional information such as the relative content of a component can be interpreted by fluorescence intensity

(FI), fluorescence index or other derived expressions. For instance, Bugden et al. (2008), used the slope ratio and the intensity ratios to interpret 3-D fluorescence data based on specific peak FI value in order to detect oil and chemically dispersed oil in seawater. 3-D fluorescence can yield important information on the chemical nature of NOM, especially for the aromatic organic materials. The aromatic carbon compounds can yield the carbonaceous DBPs, such as trihalomethanes (THMs), trichloroacetic acid and other (C-DBPs) (Hong et al., 2013). Fulvic acid also has a significant impact on the formation of THMs, haloacetic acids, and aldehydes, while 2,3,5-tribromopyrrole can be produced from humic acid (Richardson et al., 2003). This implies that there should be a relationship between the fluorescence fractions and TOC or DBPs. Humic-like fluorescence was correlated with DOC in marine DOM (Wu et al., 2007).

Compared with 2D fluorescence, the main difference with EEM is that changes in the fluorescence intensity information for the excitation and emission can be obtained simultaneously. Contour fluorescence spectrograms or 3D projections are commonly used to display EEM data. The first application of an EEM to analyze the fluorescence characteristics of DOM dates to 1990. Currently, EEM is the main method used to characterize the source, composition, and other information of DOM. However, EEMs containing multi-dimensional information are often difficult to analyze to achieve the research objectives (Jing et al., 2022; Li et al., 2020; Sgroi et al., 2017a, 2020a, 2020b).

Chen et al. (2003) employed the fluorescence regional integration method (FRI) for quantifying spectra for DOM in which the normalized fluorescence volume was used. In this important research, EEM was subdivided into different zones to characterize the different types of fluorophores in DOM. In particular, the EEM are subdivided in:

- Zone 1 (Em 280-320 nm; Ex 220-250 nm): aromatic protein, tyrosine;
- Zone 2 (Em 325-390 nm; Ex 220-250 nm): aromatic protein, BOD_5.
- Zone 3 (Em 395-580 nm; Ex 220-300 nm): fulvic acid-like substances;
- Zone 4 (Em 280-390 nm; Ex 255-300 nm): soluble microbial by-products-like substances, tryptophan, protein-like material;
- Zone 5 (Em 280-580 nm; Ex 305-450 nm): humic acid-like substances.

For every zone some index can be estimated to interpret the data. Moreover, normalized excitation–emission area volumes beneath each region can express the contents of each region. In this way, the representation of the type of substance and percent fluorescence response, can show the relative content of each sort of substance in the sample.

Overall, the most relevant methods used for the interpretation of EEM are:

- peak picking method, in which we can extract a few major information related to EEM using partial data;
- fluorescence regional integration (FRI) that calculate the total fluorescence intensities integrating the volume under the whole EEM surface for each sample;

- parallel factor analysis method (PARAFAC) based on mathematical deconvolution of fluorescence peaks.

All these methods are summarized by Hu et al. (2024) and Jing et al. (2022). Researchers have found that the PARAFAC method is very useful since it shows a more accurate estimate of the signal sources and respective contributions (Li et al., 2020). The PARAFAC model has shown a stronger linear correlation between fluorophores and DBPs formation, making it a good approach to monitoring the formation of DBPs during drinking water treatments. Table 3 shows the 3D fluorescence-based surrogates used to monitor NOM reactivity and DBPs formation in drinking water.

Table 3. Summary of 3D fluorescence-based surrogates used to monitor NOM reactivity and DBPs formation in drinking water

Method / Index	Description	Application
Fluorescence Intensity (FI = F470/F520)	Distinguishing sources of dissolved organic matter (DOM), assessing water quality indicators, predicting DBP formation.	(Jing et al., 2022; Korshin et al., 2018)
Biological Index (BIX = F380/F430)	Indicating influence of biological sources in DOM, distinguishing microbial or terrestrial sources.	(Jing et al., 2022; Korshin et al., 2018)
Humification Index (HIX)	Ratio between the average light intensity in the range from 435 to 480 nm and from 300 to 345 nm when the excitation wavelength is 245 nm. Indicating degree of humification or humic character, distinguishing DOM sources, assessing water quality indicators.	(Jing et al., 2022; Korshin et al., 2018)
Peak Picking Method	Extraction of key information related to excitation-emission matrix using partial data. Identifying key components in fluorescence spectra, investigating DBP reduction after treatment processes.	(Hu et al., 2024; Jing et al., 2022; Li et al., 2020; Nguyen et al., 2023)
Principal Components Analysis (PCA)	Semiquantitative analysis based on algorithms translating high-dimensional information into lower dimensions or reducing the number of variables. Predicting DBP formation, identifying representative substances of each component in fluorescence spectra.	(Hu et al., 2024; Jing et al., 2022; Li et al., 2020; Nguyen et al., 2023)
Parallel Factor Analysis (PARAFAC)	Analysis based on algorithms processing EEM data, separating components and indicating type and source of DBP precursors. Estimating signal sources and contributions, predicting DBP formation, monitoring DBPs during water treatment processes.	(Hu et al., 2024; Jing et al., 2022; Li et al., 2020; Nguyen et al., 2023)
Artificial Neural Network (ANN)	Machine learning approach using fluorescence parameters from PCA and PARAFAC as input to predict DBP precursors. Improving prediction accuracy, monitoring drinking water quality using artificial intelligence methods.	(Nguyen et al., 2023)
I_1	Intensity fluorescence zone 1 (Em 280-320 nm; Ex 220-250 nm) peak. Indicates the presence of aromatic proteins.	(Chen et al., 2003; Jing et al., 2022; Li et al., 2020; Nguyen et al., 2023; Yang et al., 2008)

I_2	Intensity fluorescence zone 2 (Em 325-390 nm; Ex 220-250 nm) peak. Indicates the presence of BOD5.	(Chen et al., 2003; Jing et al., 2022; Li et al., 2020; Nguyen et al., 2023; Yang et al., 2008)
I_3	Intensity fluorescence zone 3 (Em 395-580 nm; Ex 220-300 nm) peak. Indicates the presence of fulvic acid substances.	(Chen et al., 2003; Jing et al., 2022; Li et al., 2020; Nguyen et al., 2023; Yang et al., 2008)
I_4	Intensity fluorescence zone 4 (Em 280-390 nm; Ex 255-300 nm) peak. Indicates the presence of microbiological soluble products or amino acids like Tryptophan.	(Chen et al., 2003; Jing et al., 2022; Li et al., 2020; Nguyen et al., 2023; Yang et al., 2008)
I_5	Intensity fluorescence zone 5 (Em 280-580 nm; Ex 305-450 nm) peak. Associated with humic acid substances.	(Chen et al., 2003; Jing et al., 2022; Li et al., 2020; Nguyen et al., 2023; Yang et al., 2008)
ϕ_I	The volume beneath region 1 of the EEM. Represent the cumulative fluorescence response of DOM with similar properties.	(Chen et al., 2003; Yang et al., 2008)
ϕ_{II}	The volume beneath region 2 of the EEM. Represent the cumulative fluorescence response of DOM with similar properties.	(Chen et al., 2003; Yang et al., 2008)
ϕ_{III}	The volume beneath region 3 of the EEM. Represent the cumulative fluorescence response of DOM with similar properties.	(Chen et al., 2003; Yang et al., 2008)
ϕ_{IV}	The volume beneath region 4 of the EEM. Represent the cumulative fluorescence response of DOM with similar properties.	(Chen et al., 2003; Yang et al., 2008)
ϕ_V	The volume beneath region 5 of the EEM. Represent the cumulative fluorescence response of DOM with similar properties.	(Chen et al., 2003; Yang et al., 2008)

3.0 IDENTIFICATION OF FLUORESCENCE INDEXES SUITABLE FOR SENSOR DEVELOPMENT

3.1 *EEM of water samples from Case Studies*

As reported in the prior section (§2), fluorescence EEM can be considered as a fingerprint of a water sample. In particular, EEM gives information about the presence of fluorophores, which are the substances that emit fluorescence. The fluorophore's presence and intensity give information on which DOM fraction, qualitatively and quantitatively, can be found in the sample. As reported in the literature (§2), fluorescence EEM can also give information on the content and reactivity of DOM in DBP formation.

The removal of EEM during the treatment trains at a DWTP indicates the removal of DOM and DBP precursors. For instance, Figure 1 shows the decrease of fluorescence EEM over the treatment train at the CS-1. As expected, the decrease in EEM is significant during the DWTP, while from the outlet to the distribution system, the changes in EEM are less significant. A similar trend can be observed for the EEMs of waters collected at the DWTP and distribution system in CS-2 (Figure 2) and in CS-3 (Figure 3).

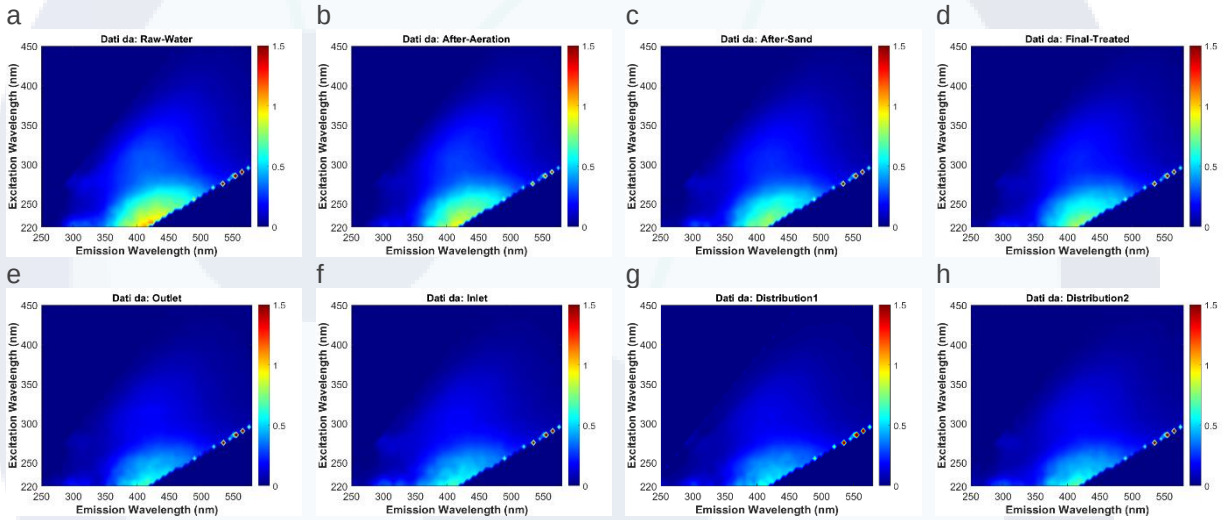


Figure 1. EEM of CS-1 (Limassol) samples collected at different points: a) Raw water, b) Post Aeration, c) Post Sand Filter, d) Final treated, e) Outlet, f) Inlet, g) Distribution 1, h) Distribution 2

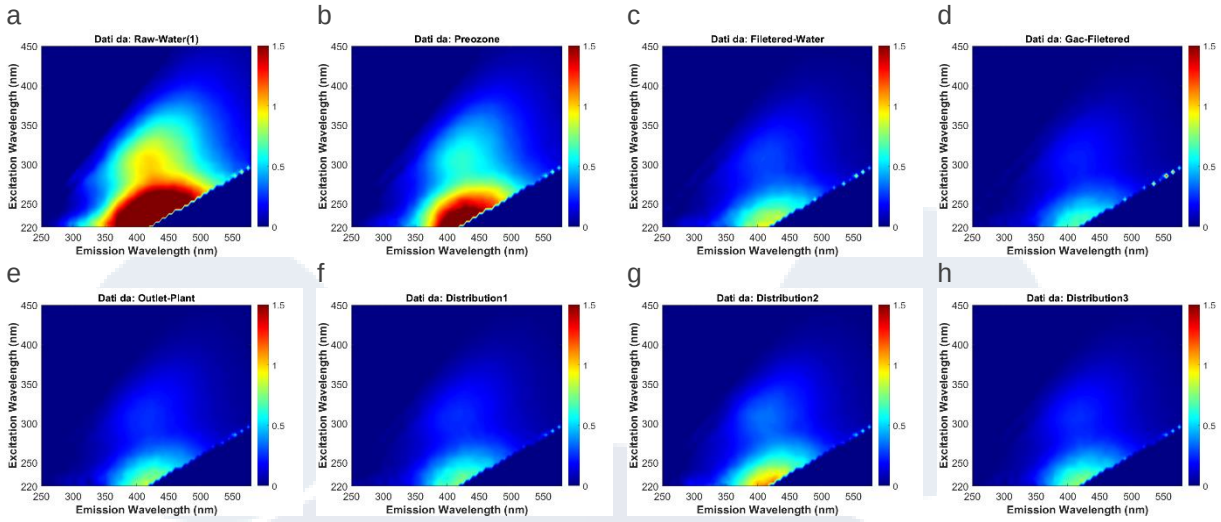


Figure 2. EEM of CS-3 (Madrid) samples collected at different points: a) raw water, b) Pre Ozone, c) Post Filter, d) Post Activated Carbon, e) Outlet, f) Distribution 1, g) Distribution 2, h) Distribution 3

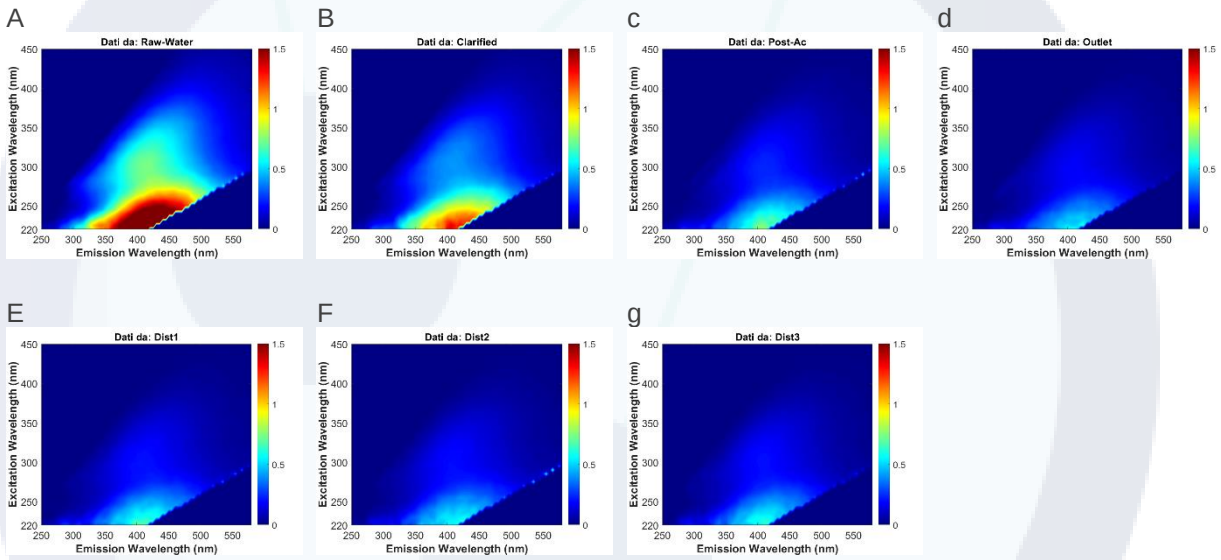


Figure 3. EEM of CS-2 (Barcelona) samples collected at different points: a) raw water, b) Post clarified, c) Post AC, d) Outlet, e) Distribution 1, f) Distribution 2, g) Distribution 3

3.2 Correlations between fluorescence indexes and DBPs

3.2.1 DBPs Formation Potential prediction

To find a specific fluorescence ex/em pair that can be used to predict DBP formation during chlorination, several literature data and UCT own data have been used. Two indexes have been selected from EEM data as indicators of NOM reactivity in DBPs formation, namely I3 (255,440) and I5 (325,450), which are representative of fluvic- and humic-like material, respectively. These two indexes have been found to correlate with DBPFP in chlorinated waters. For instance, Figure 4 shows a correlation between either ΔI3 or ΔI5 and the DBPFP obtained from chlorination of ATL water samples collected at different points of the DWTP on two different sampling days. The determination coefficients obtained for ΔI3 or ΔI5 indexes are very high, especially for HAA5 and HAA9, while for THM are lower. The high correlation is due to the fact that the changes in I3 or I5 during chlorination, measured by the differential approach (Roccaro et al., 2009; Roccaro and Vagliasindi, 2009) is related to the halogenation process and subsequent release of DBPs (Zhang et al., 2021). Furthermore, also the absolute values of such fluorescence indexes I3 and I5 are correlated with DBPFP with similar determination coefficients to those observed for the differential indexes (Figure 5). The latter result is very important because could allow monitoring of the NOM reactivity during the DWTP with online sensors.

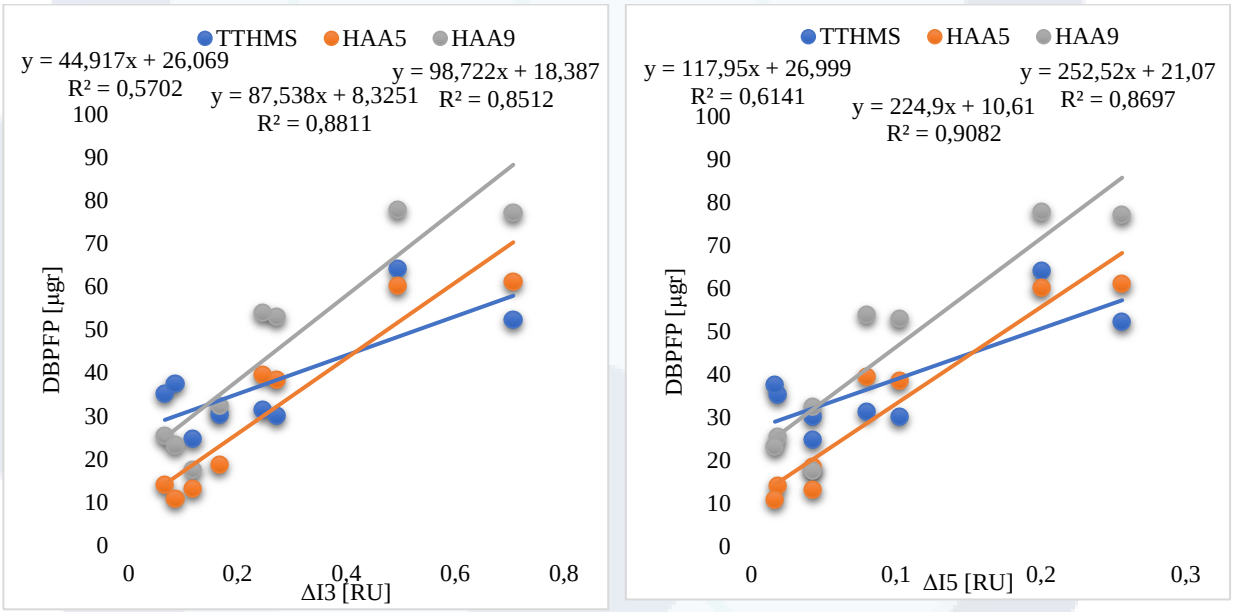


Figure 4. Correlation between ΔI3 or ΔI5 and DBPFP in chlorinated ATL (CS-2) waters (raw, clarified, GAC filtered, outlet) in two different sampling days

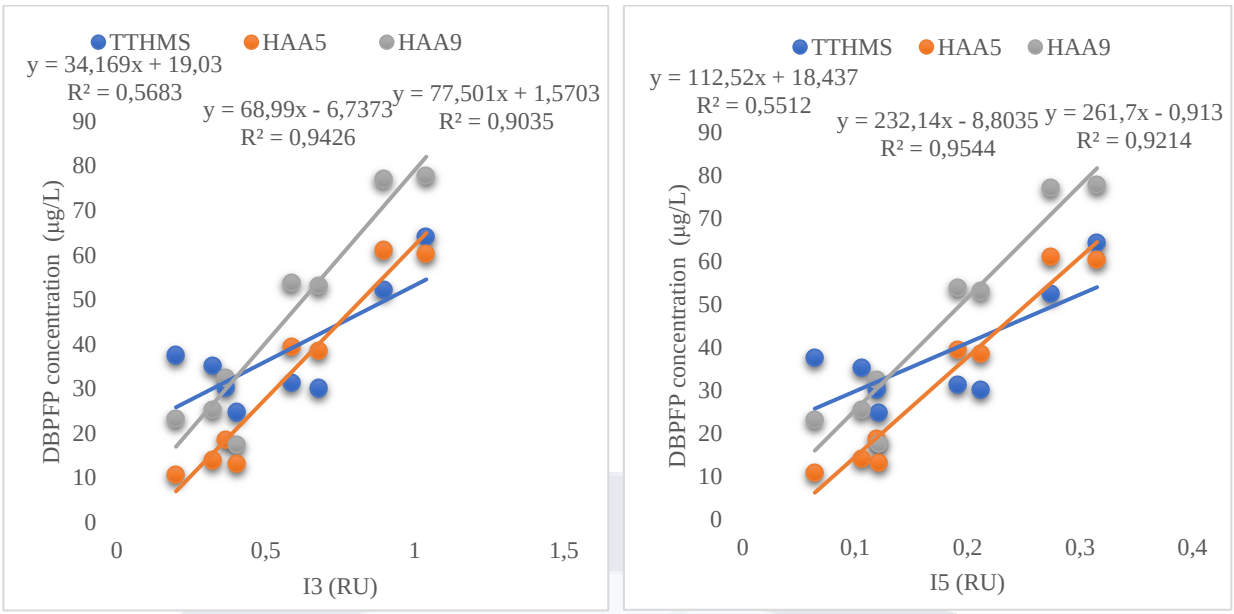


Figure 5. Correlation between I3 or I5 and DBPFP in chlorinated ATL (CS-2) waters (raw, clarified, GAC filtered, outlet) in two different sampling days

3.2.2 DBPs concentration monitoring

The selected fluorescence indexes I3 and I5 have been used also to track the DBP concentrations measured in the water collected at the CSs along the DWT and distribution system. Obtained results are more complex to interpret due to the several factors affecting the DBPs concentration, such as the amount of chlorine dosed, the reaction time, and the precursors removal. In some cases, the I3 and I5 data were well correlated with the DBPs concentrations as reported in Figure 6 for TTHMs in CS-3 waters.

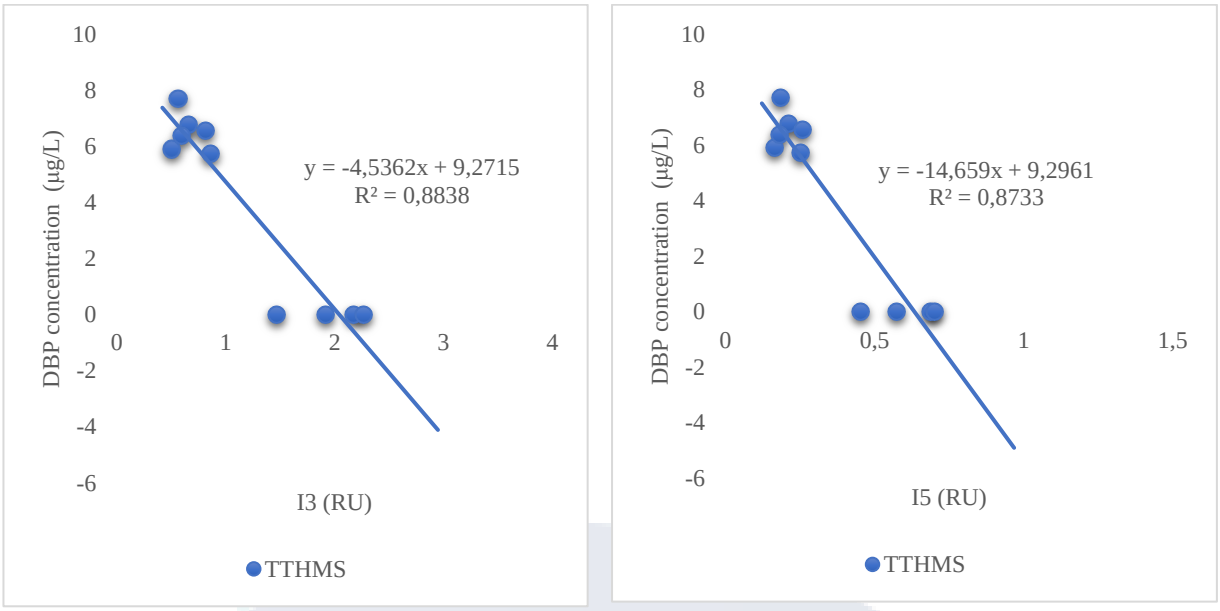


Figure 6. Correlation between I3 and DBPFP in chlorinated Madrid (CS-3) waters (raw, pre-ozonated, sand filtered, GAC filtered, outlet) in two different sampling days

4.0 CORRELATIONS BETWEEN FLUORESCENCE MEASUREMENTS OBTAINED FROM SPECTROFLUOROMETER AND CUSTOMIZED SENSOR

A sampling campaign was planned for each case study to perform the sensor calibration on several reference waters and investigate the use of fluorescence sensors for DBPs control before the online implementation. The customized fluorescence sensors employed in this study worked in conjunction with a Photometric Transmitter (PT) through a fiber optic cable. Therefore, each PT was connected to the related probe and equipped with optical filters to provide a specific excitation/emission wavelength pair ($\lambda_{ex}/\lambda_{em}$). The excitation/emission pairs were selected according to the findings highlighted in the previous section (Table 4).

Table 4. Excitation/emission pair of fluorescence sensors investigated in this project

Sensor	λ_{ex}	λ_{em}
I3	257	440
I5	325	448

Water samples were taken in 125 mL amber brown HDPE bottles to protect samples from UV/VIS light and ensure dark conditions for reliable fluorescence measurements. A computer was connected to the PT for real-time data transfer. The data logging settings were regulated by two main parameters: measurement interval (approximately 2-3 min), that is the time window in which fluorescence data is to be obtained; logging interval (set to 5 sec), which represents how often data will be saved to the log file during the measurement interval. The average value of fluorescence intensities obtained every 5 s for each sample was considered as a representative value of that sample.

4.1 Calibration of fluorescence sensors

Before starting the fluorescence measurements of a given set of samples, a calibration of the sensors (“autotune”) is required. As a preliminary step, sensors were tested with different water matrices collected and analyzed by UCT team. Initially, fluorescent sensors were calibrated by taking as reference a raw sample from surface waters located in Catania (IT). Measurements were carried out on four linearly diluted samples of each tested water, blending the raw sample with DI water with concentrations (v/v) from 75% to 0%. Then the autotune for sensor calibration was performed on the five samples including the raw water and the four diluted samples of the case studies (CSs). For instance, Figure 7 shows the calibration results obtained by the water samples from CS-

1 (Limassol, Cyprus) and CS-3 (Canal, Spain). Fluorescence intensities are given in Arbitrary Units (AU).

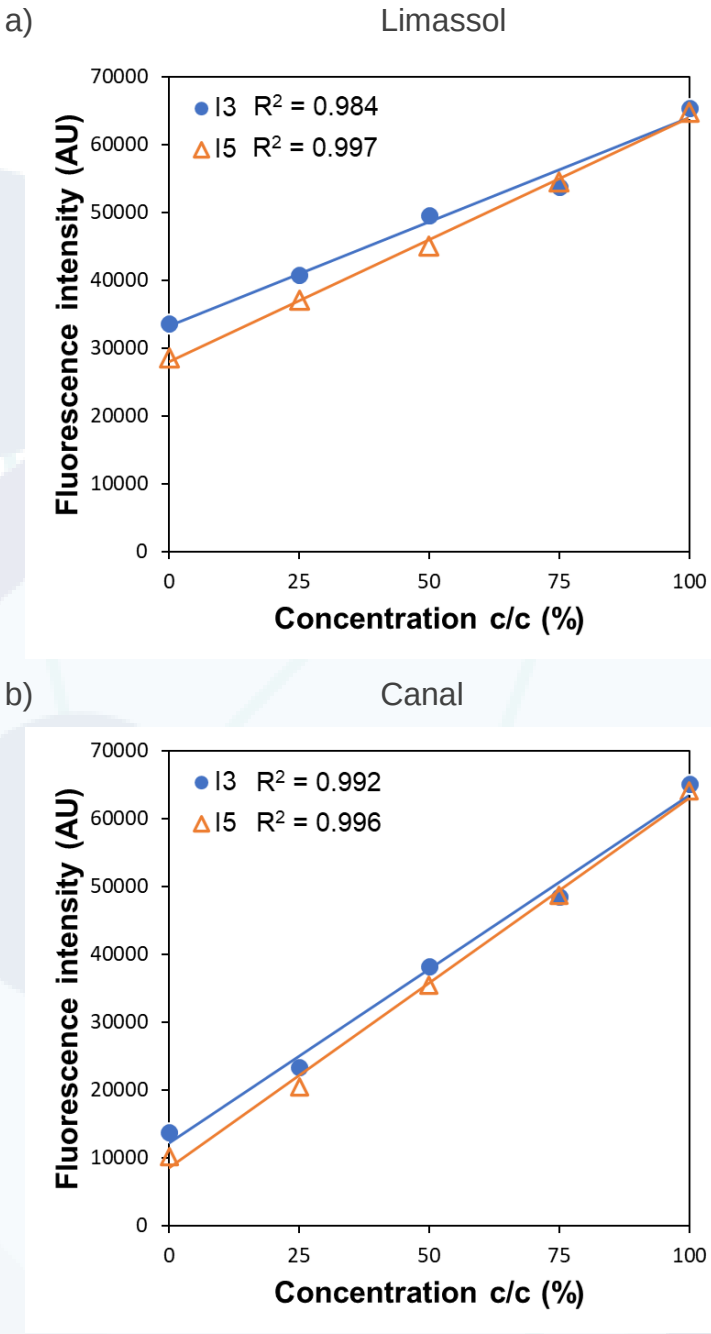


Figure 7. Calibration lines of the five fluorescence sensors on Limassol (a) and Canal (b) raw waters

4.2 Fluorescence sensors validation

4.2.1 Validation of fluorescence sensors with different water matrices

The selected fluorescence sensors were validated by correlating the data obtained from the laboratory spectrofluorometer (Shimadzu RF-5301PC) and those obtained by the sensor fluorescence. The fluorescence intensities obtained from the laboratory spectrofluorometer were extracted from the 3-D EEMs and elaborated to obtain fluorescence raw data (Arbitrary Units, AU) and corrected data by inner filter effect (IFE) and blank corrections, and Raman normalisation (Raman Units, RU).

Figure 8 shows the strong linear correlation between fluorescence sensors and lab-scale spectrofluorometer data of four diluted samples from two different surface waters collected in the Catania area. Then, fluorescence sensors I3 and I5 were tested with different water matrices, including surface water, and tap water to investigate the sensor sensitivity before validating the sensors with water samples from case studies. As shown in Figure 9, a very strong linear correlation was found for both I3 and I5 sensors regardless of the type and content of DOM.

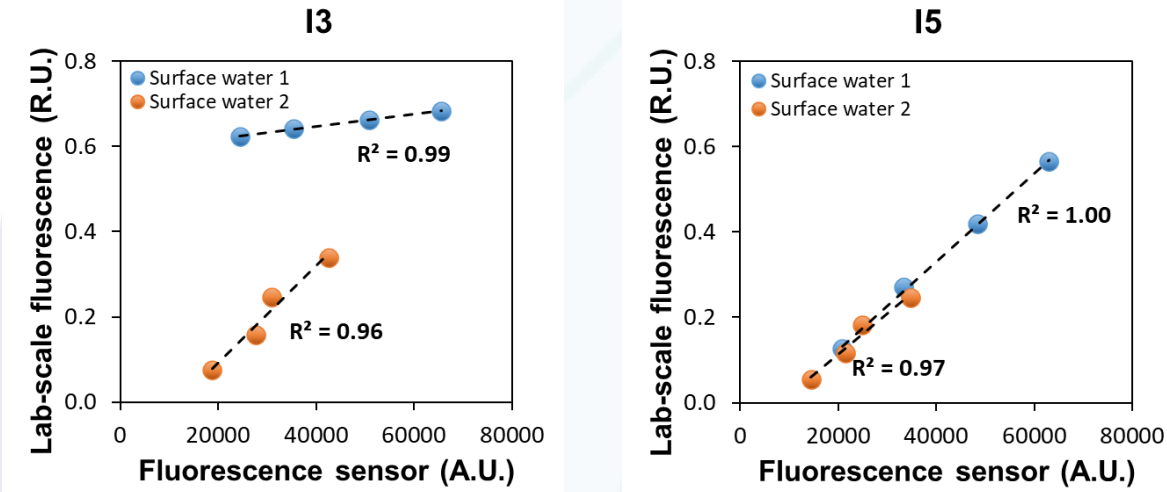


Figure 8. Linear correlation between fluorescence indexes measured by sensors and lab-scale spectrofluorometers of four diluted samples of two different surface waters

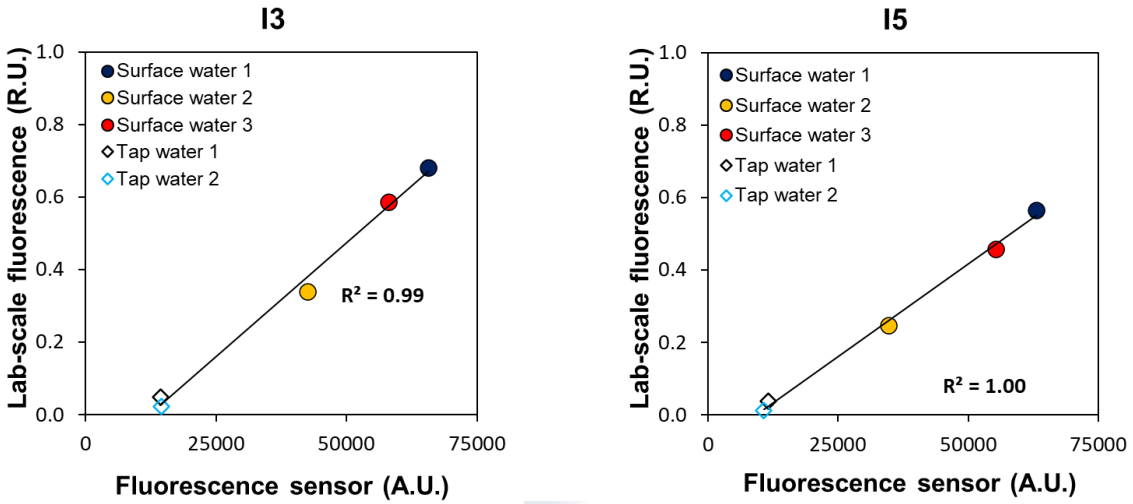


Figure 9. Linear relationship between fluorescence measurements by sensors and lab-spectrofluorometer for a set of different water matrices

In the following sections the linear correlation between lab-fluorometer and sensor fluorescence data will be reported for each case study.

4.2.2 Validation of fluorescence sensors on samples from CS-1 (Limassol, Cyprus)

UCY carried out 3 sampling campaigns on February, March and April 2024, collecting 1 L of raw water for sensor calibration, and the following 8 samples along the DWTP and distribution network:

1. DWTP Outlet (sensor station)
2. Zone 2 inlet
3. Zone 2 outlet (sensor station)
4. DMA Inlet (sensor station)
5. Distribution Point 1
6. Distribution Point 2
7. Distribution Point 3 (sensor station)
8. Distribution Point 4

The location of the 8 sampling points is reported in Figure 10.

Samples were collected with and without quenching agent (sodium sulfite) to evaluate the effect of such quencher on the fluorescence signals. As expected, quenched samples showed higher fluorescence in both cases (lab-fluorometer and sensors). Lab-fluorescence analysis was performed on each sample to obtain the EEMs, following the established procedures by UCT in previous works (Sgroi et al., 2018, 2017b). As an example, Figure 11 and Figure 12 illustrates the EEMs of non-quenched and quenched samples (February sampling campaign), respectively. Data are shown in RU in both cases. In general, an increase in fluorescence intensity could be noted in quenched samples for all EEM regions.

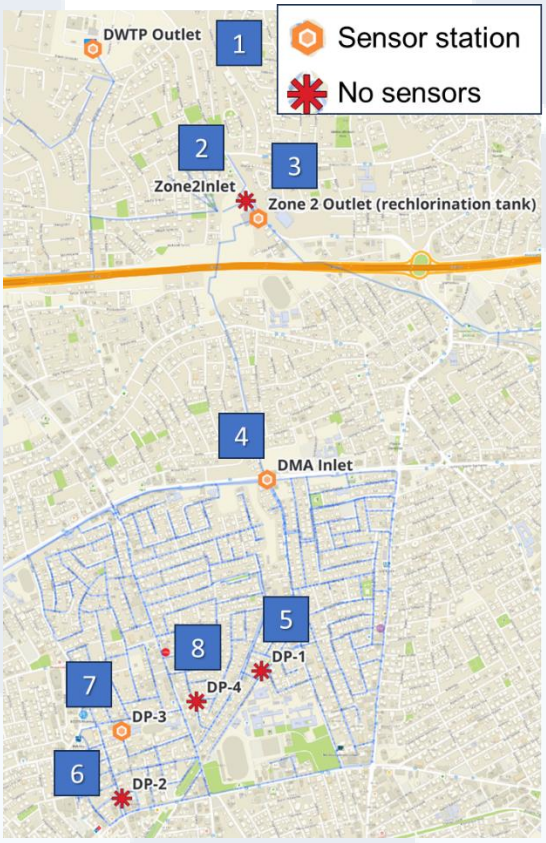


Figure 10. Location of sampling point for the CS1 (Cyprus) case study

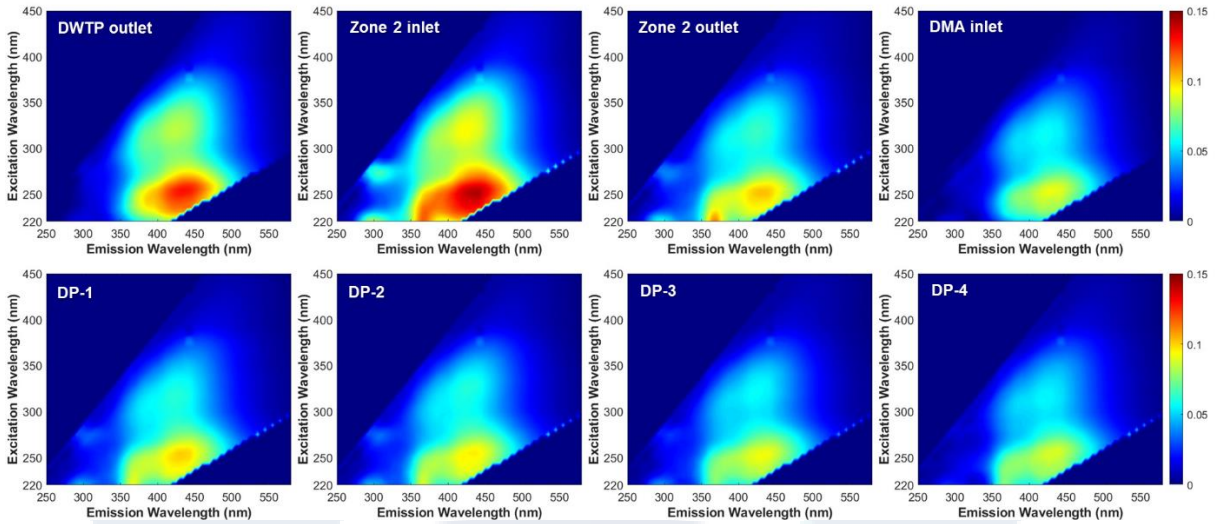


Figure 11. Fluorescence EEMs of non-quenched samples from the Cyprus case study (February sampling campaign)

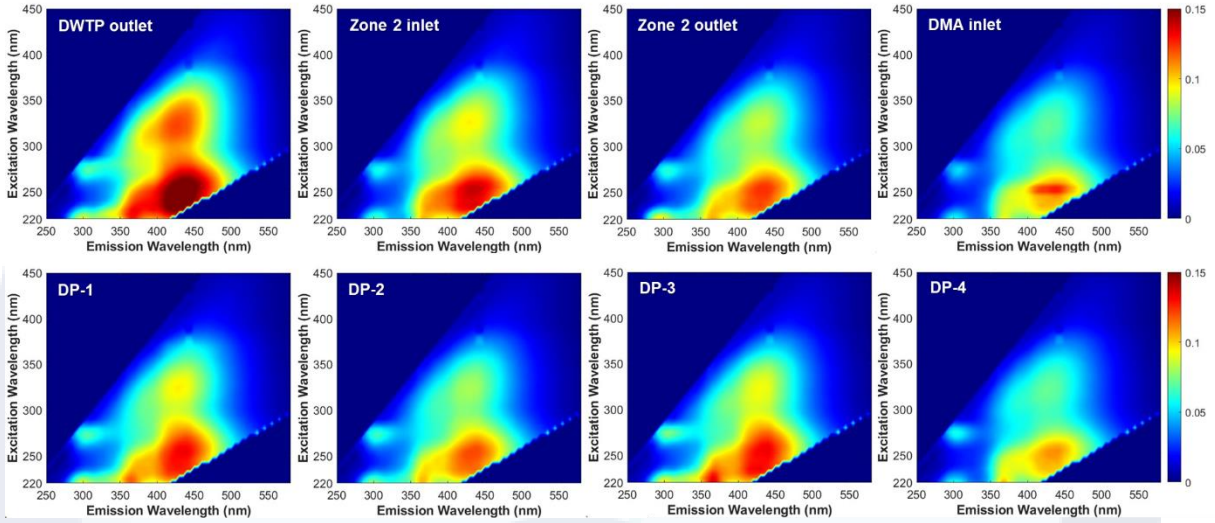


Figure 12. Fluorescence EEMs of quenched samples from the Cyprus case study (February sampling campaign)

Furthermore, Figure 13 shows the differences in fluorescence intensities of peaks I3 and I5 of quenched and not-quenched samples.

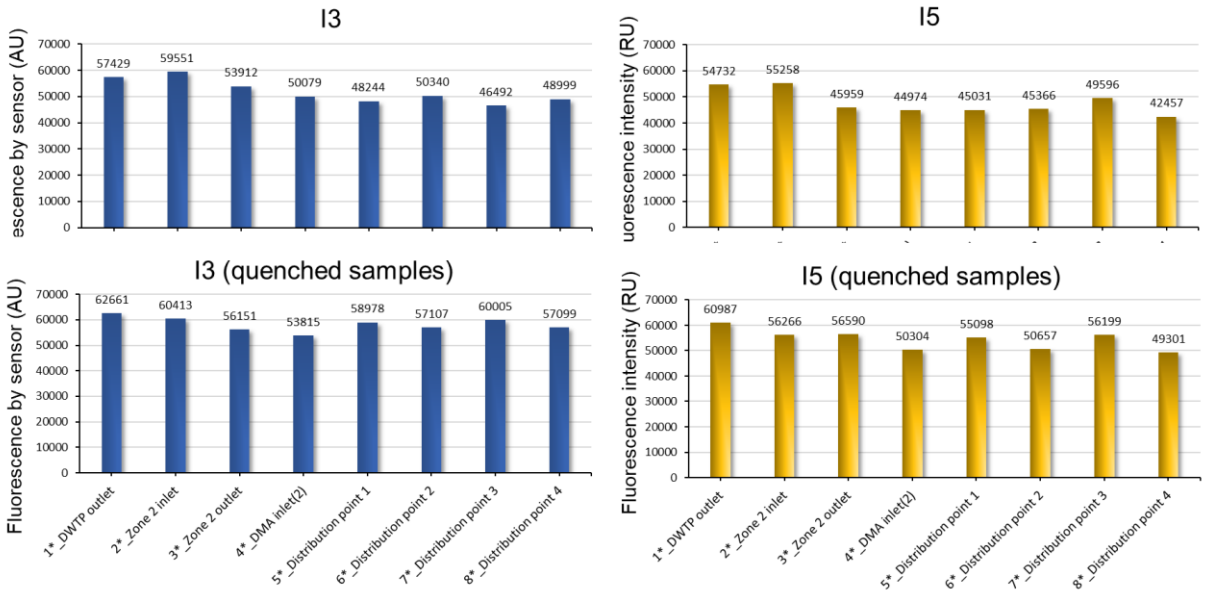


Figure 13. Fluorescence intensities obtained with I3 and I5 sensors from quenched and not-quenched samples from CS-1

The fluorescence parameters from the EEM were calculated for each sample and compared with the fluorescence sensor data, developing linear correlations for quenched and not-quenched samples. The fluorescence intensity obtained by peak-picking method in Arbitrary Units was the best correlated with sensor fluorescence data. As an example, Figure 14 depicts the linear correlations for samples of the February sampling campaign.

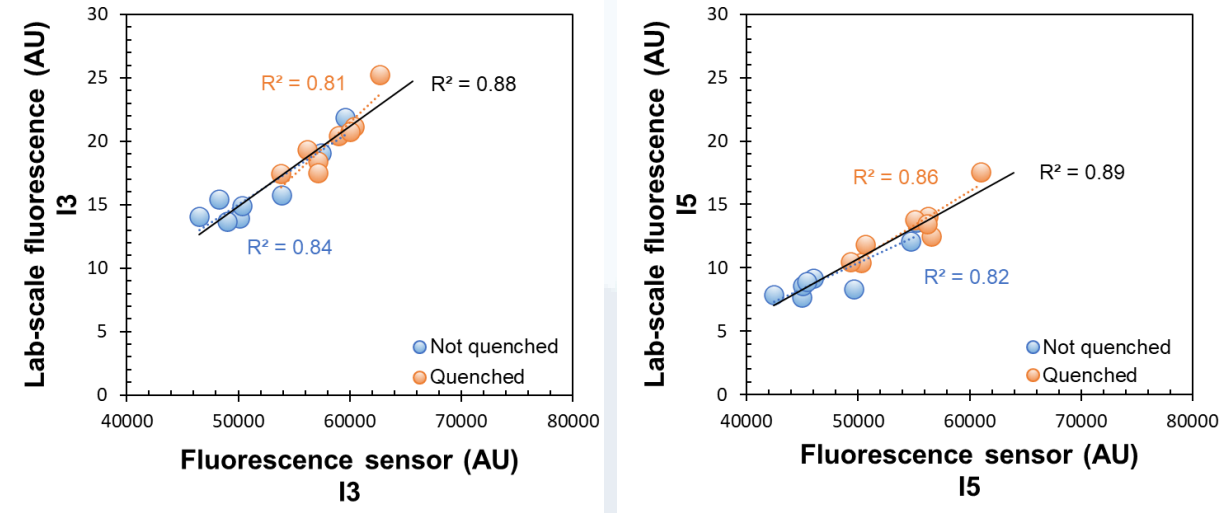


Figure 14. Linear correlation between the values of fluorescence intensity I3 or I5 obtained by the spectrofluorometer (Arbitrary Units) and the fluorescence signals from sensors I3 or I5 for CS-1

It could be noted that quenched and not-quenched samples follow the same regression line. In general, very high correlations were found between fluorescence by the sensor and lab-fluorometer for both I3 and I5 peaks, validating the measures gained with the sensor.

4.2.3 Validation of fluorescence sensors on samples from CS-2 (Barcelona, Spain)

A set of 7 samples from several points of the water treatment plant (Figure 15) and distribution system was collected by ATL (CS-2) on April 2024 and sent to UCT for fluorescence analysis and sensor calibration. Following is the list of samples:

1. Raw water
2. Post clarified water
3. Post activated carbon filters (before NaClO addition)
4. Outlet of the plant (after plant tanks – blended with desalinated water)
5. Distribution system 1 (HRT = 10 h)
6. Distribution system 2 (HRT = 66 h)
7. Distribution system 3 (HRT = 113 h)

All samples were collected and shipped without adding quencher.

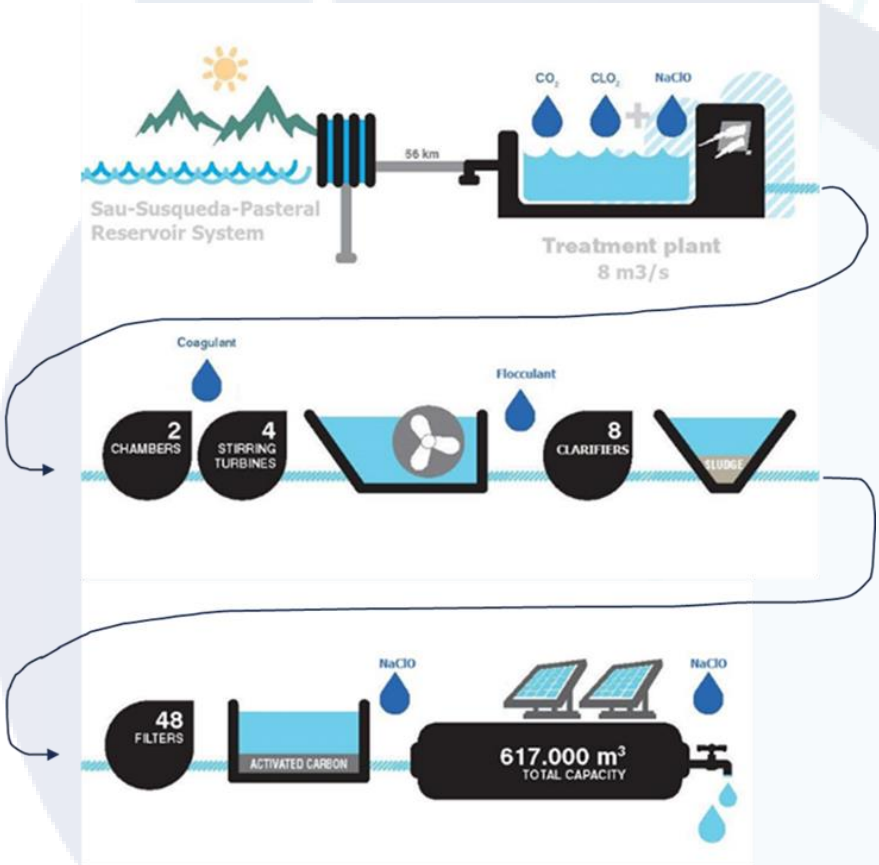


Figure 15. Simplified scheme of the DWTP managed by ATL (Barcelona case study)

Figure 16 shows the reduction of peaks I3 and I5 obtained with the sensor along the water treatment train and the distribution system.

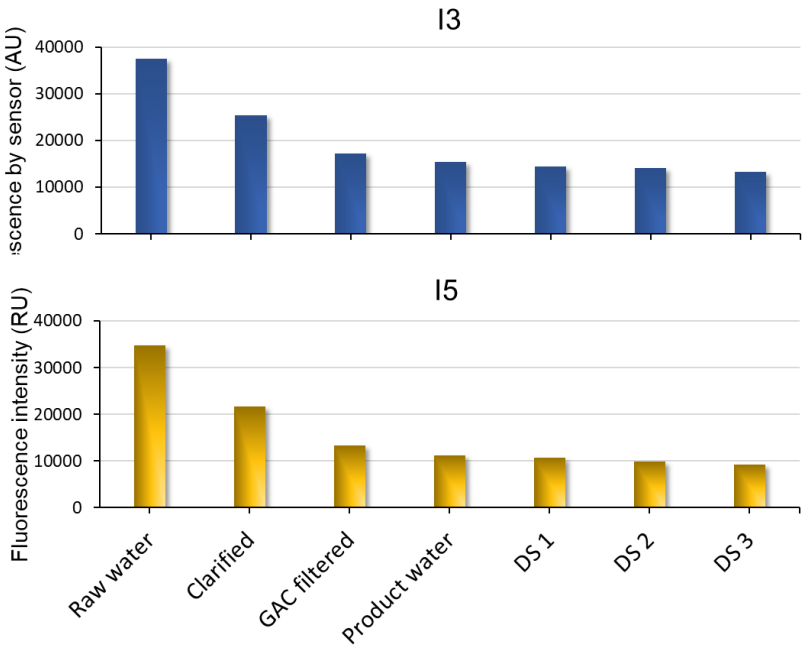


Figure 16. Reduction of fluorescence peaks (I3 and I5) by sensors during treatment stages and distribution system of water samples from CS-2

While the fluorescence intensity of I3 and I5 is quite constant in the distribution system (DS1, DS2, DS3 points), the decrease in fluorescence along the DWTP is more noticeable compared to CS-1.

Again for validation purposes, fluorescence parameters gained with lab-fluorometer were compared to fluorescence signals obtained by the sensor. For instance, Figure 17 shows the strong linear relationship between fluorescence peaks from the EEM and fluorescence by sensors. In this case, very high correlations were found for all fluorescence parameters.

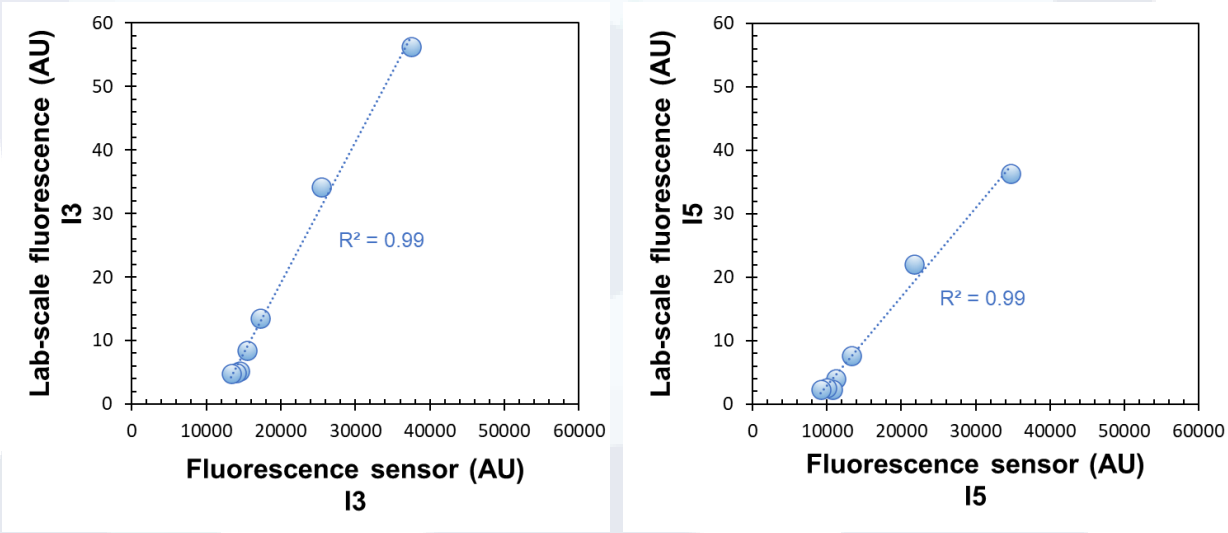


Figure 17. Linear correlation between the values of fluorescence intensity I3 or I5 obtained by the spectrofluorometer (Arbitrary Units) and the fluorescence signals from sensors I3 or I5 for CS-2

4.2.4 Validation of fluorescence sensors on samples from CS-3 (Madrid, Spain)

On April 2024 Canal collected 7 samples from different points of their DWTP (Figure 17) and distribution network that were shipped to the UCT team. The samples are as follows:

1. Raw water
2. Pre-ozoned water
3. Filtered water
4. Outlet of the plant
5. Distribution 1
6. Distribution 2
7. Distribution 3

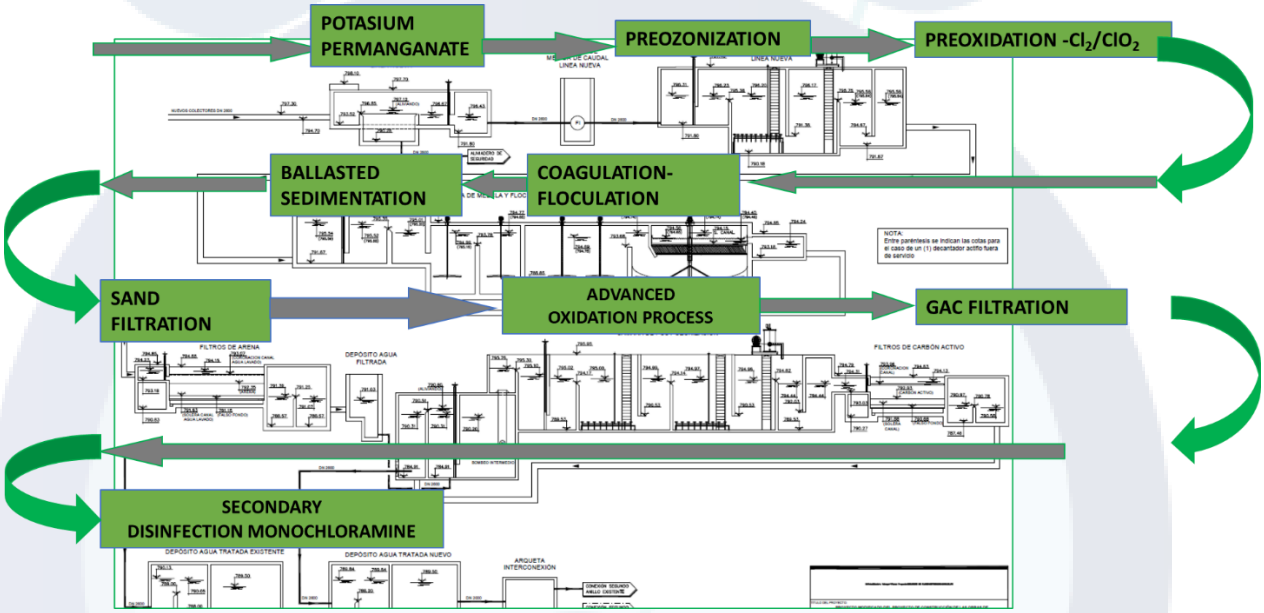


Figure 18. Simplified scheme of the DWTP managed by Canal (Madrid case study)

All samples were sent without a quenching agent. Figure 19 shows the decrease in fluorescence peaks I3 and I5 along the treatment stages and distribution network (DP1, DP2, DP3) in CS-3.

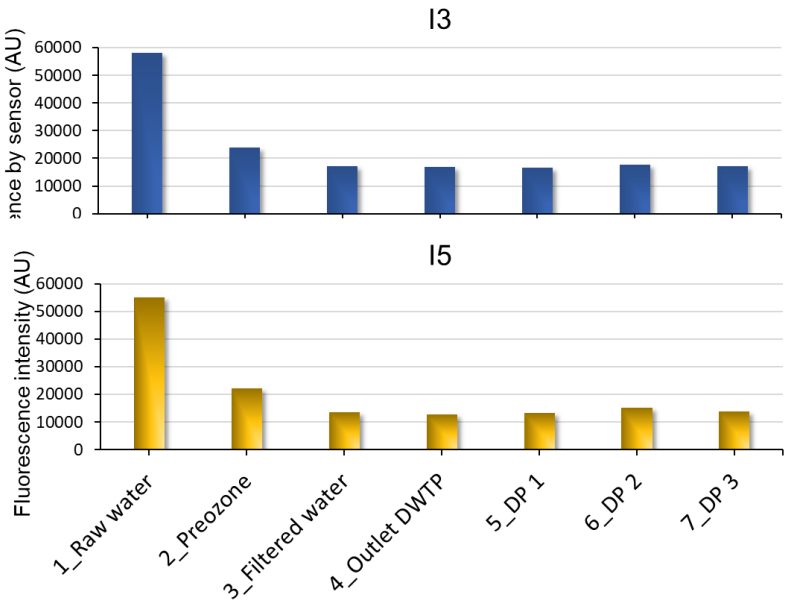


Figure 19. Reduction of fluorescence peaks (I3 and I5) by sensors during treatment stages and distribution system of water samples from CS-3

Similarly to CS-2, the reduction in fluorescence intensity of peaks I3 and I5 during DWTP was observed, while along the distribution points the fluorescence signals did not decrease monotonically as expected.

The high correlations found between all fluorescence data from the lab-fluorometer and fluorescence data from the sensors suggest the high reliability of the sensor measurements (Figure 20).

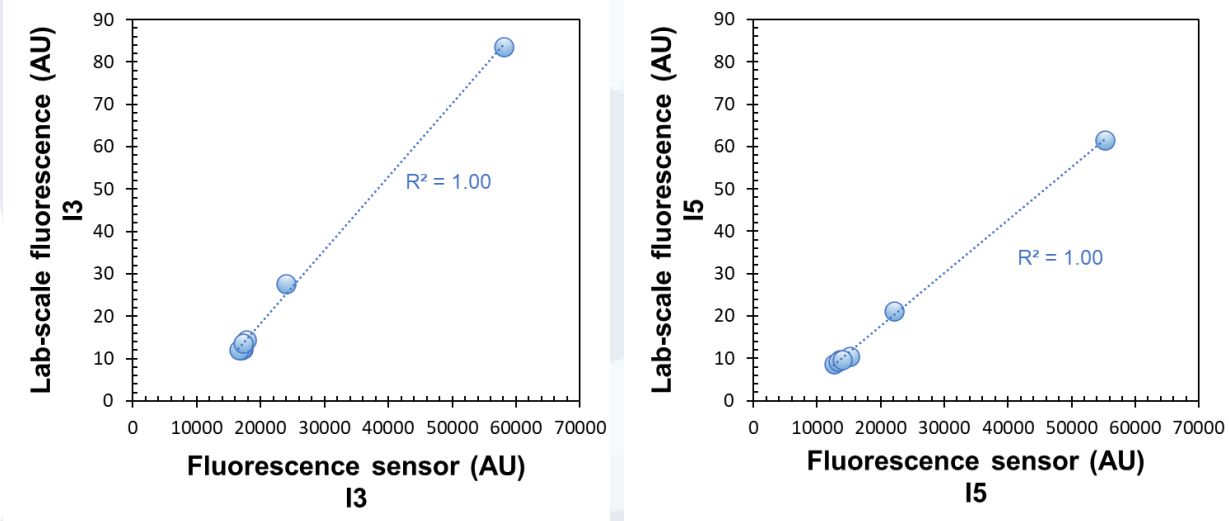


Figure 20. Linear correlation between the values of fluorescence intensity I3 or I5 obtained by the spectrofluorometer (Arbitrary Units) and the fluorescence signals from sensors I3 or I5 for CS-3

4.2.5 Validation of fluorescence sensors using all data together from CSs

The fluorescence values of the entire dataset including ATL, Canal, and Limassol (February, March, April and May sampling campaigns) obtained by the laboratory spectrofluorometer have been correlated with the corresponding fluorescence signals collected by the sensors off-line. The observed linear correlations are shown in Figure 21. Notably, the combination of ATL, Canal and Cyprus (May sampling campaign) fluorescence data results in a sole dataset of benchtop fluorescence data vs. sensors data with a very strong correlation $R^2 = 0.94$ and $R^2 = 0.98$ for I3 and I5 index, respectively. On the other hand, Cyprus datasets related to February, March and April sampling campaigns are located in a cluster with low R^2 (Figure 21). This fact could be ascribed to the different calibrations used during the measurements. Indeed, ATL, Canal and Cyprus (May) samples were analysed with sensors calibrated on the same reference water (Madrid raw water). The fact that another calibration was used for Limassol samples of February, March and April campaigns could explain the difference in the correlation pattern. Therefore, in order to facilitate the fluorescence data comparison of different water matrices, it is highly recommended to consider data obtained with the same calibration. These findings are in accordance with preliminary results illustrated in Figure 9, in which fluorescence data of different waters obtained with the same calibration lay on the same regression line.

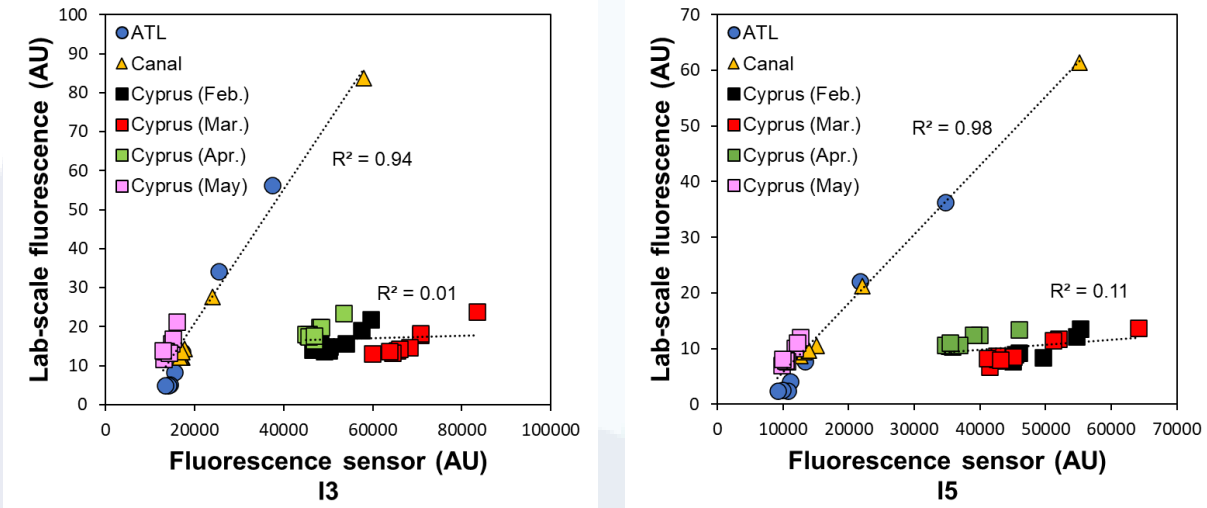


Figure 21. Linear correlation between the values of fluorescence intensity I3 or I5 obtained by the spectrofluorometer (Arbitrary Units) and the fluorescence signals from sensors I3 or I5 for all CSs data together (CS-1+CS-2+CS-3)

5.0 CORRELATIONS BETWEEN FLUORESCENCE SENSORS SIGNALS AND DBPs

5.1 DBP Formation Potential (DBPFP)

The ability of the fluorescence sensors to measure the NOM reactivity in DBPs formation was investigated. For this reason, chlorinated samples from CS-1 were sent to UCT for fluorescence sensor analysis. In particular, samples for formation potential (FP) analysis were collected from the Limassol (UCY) distribution system during three different sampling campaigns carried out in February, March and April 2024. Sampling points were as follows:

1. DWTP outlet
2. Zone 2 inlet
3. Zone 2 outlet
4. DMA inlet

Figure 22 shows the THMFP at the different points of the distribution system. The THMFP values show that the brominated species are present and that the reactivity of the water in THM formation is similar. This is expected because all the sampling points are located downstream of the DWTP and therefore there is not a significant removal of NOM.

Figure 23 shows the linear correlation models between fluorescence signals from sensors I3 or I5 and THMFP data obtained by the chlorination of Limassol water collected during the March sampling campaign. In general, low R^2 were found, but some THMs showed good correlations with the fluorescence of the I3 and I5 sensors (e.g., BDCM and DBCM).

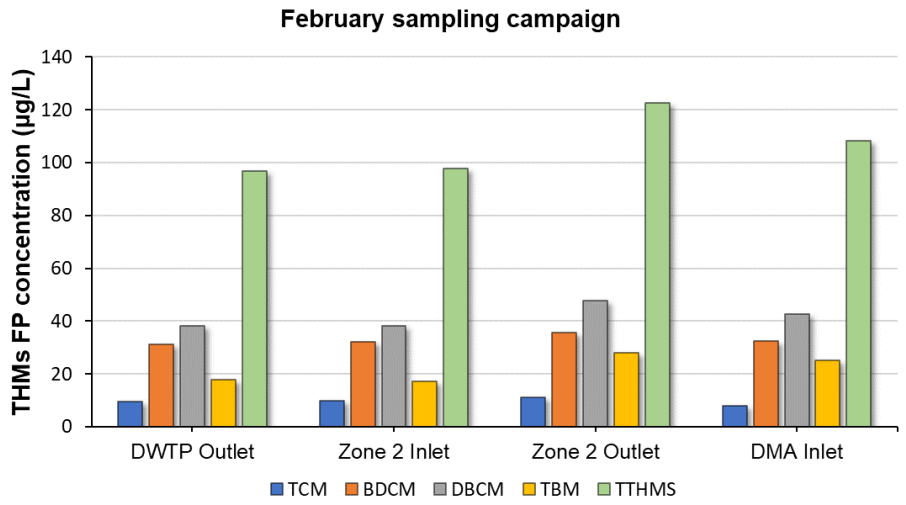
Further linear correlation modes were developed using the differential fluorescence measured as:

$$\Delta I_{FP} = I - I_{FP}$$

where I is the fluorescence peak measured in samples without chlorine addition, and I_{FP} is the fluorescence peak measured in samples chlorinated for formation potential tests.

Correlations between ΔI_3 or ΔI_5 and THMFP are illustrated in Figure 24. Such correlations are higher than those observed for I3 or I5. This could be explained because the changes in fluorescence during chlorination are related to fluorophores that react with chlorine to form THMs. However, the application of the ΔI_{FP} in real WTP or distribution systems is more complex than using the absolute I3 or I5 values.

a)



b)

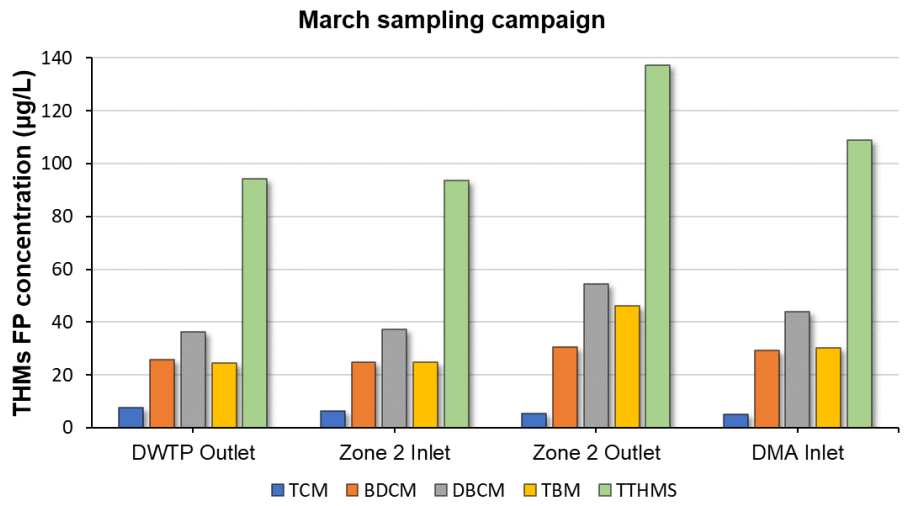
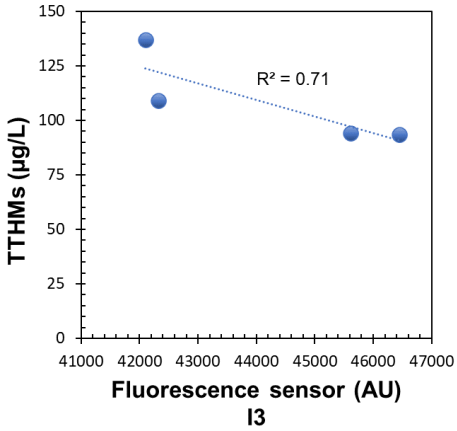
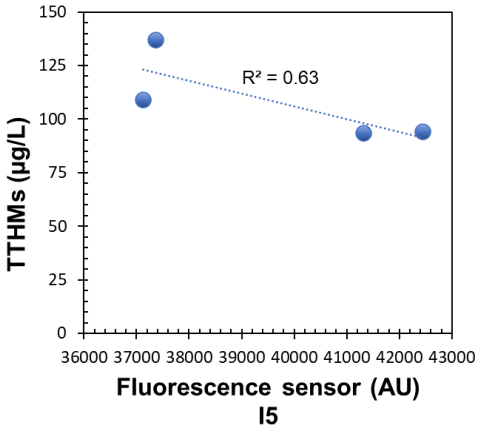
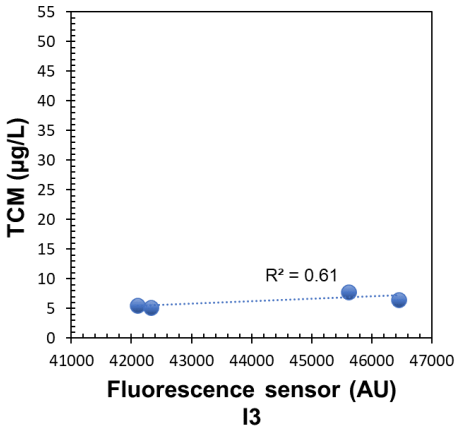
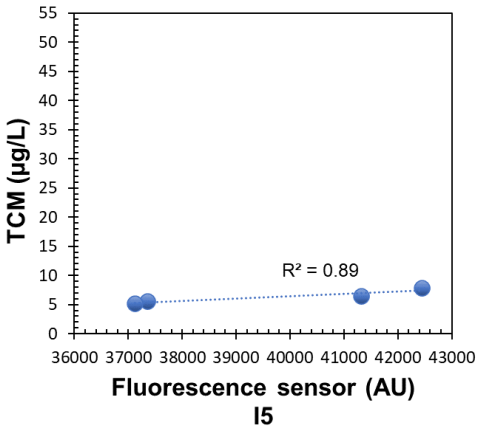


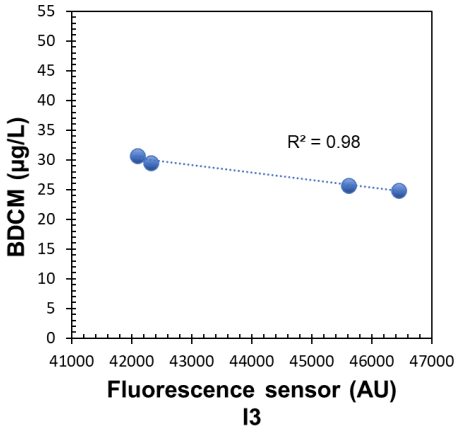
Figure 22. THMs concentration detected in Cyprus water samples from FP tests carried out on February (a) and March (b) sampling campaigns

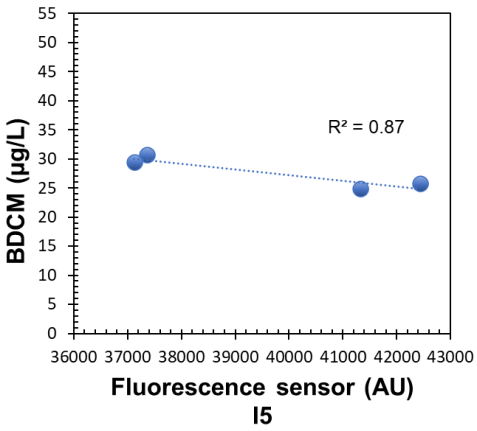

TTHMs (µg/L)
R² = 0.71
Fluorescence sensor (AU)
I3


TTHMs (µg/L)
R² = 0.63
Fluorescence sensor (AU)
I5


TCM (µg/L)
R² = 0.61
Fluorescence sensor (AU)
I3


TCM (µg/L)
R² = 0.89
Fluorescence sensor (AU)
I5


BDCM (µg/L)
R² = 0.98
Fluorescence sensor (AU)
I3


BDCM (µg/L)
R² = 0.87
Fluorescence sensor (AU)
I5

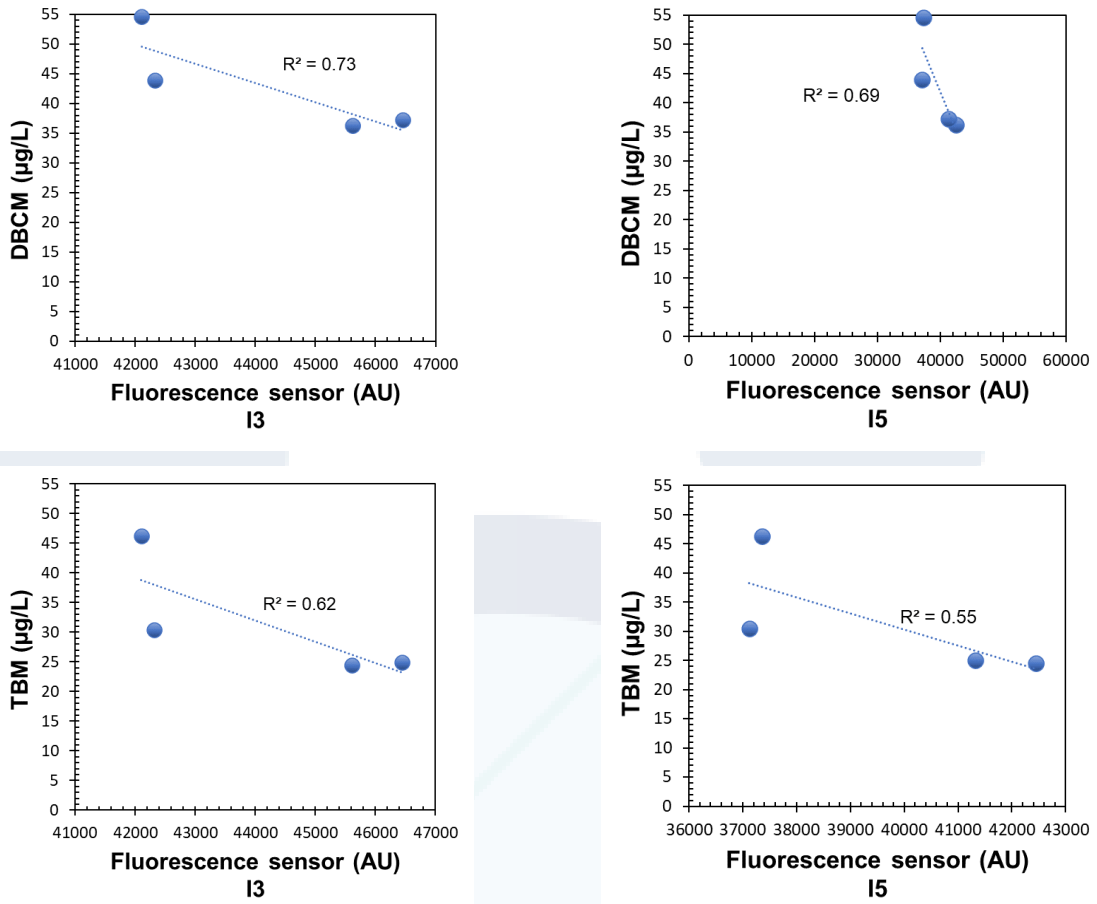
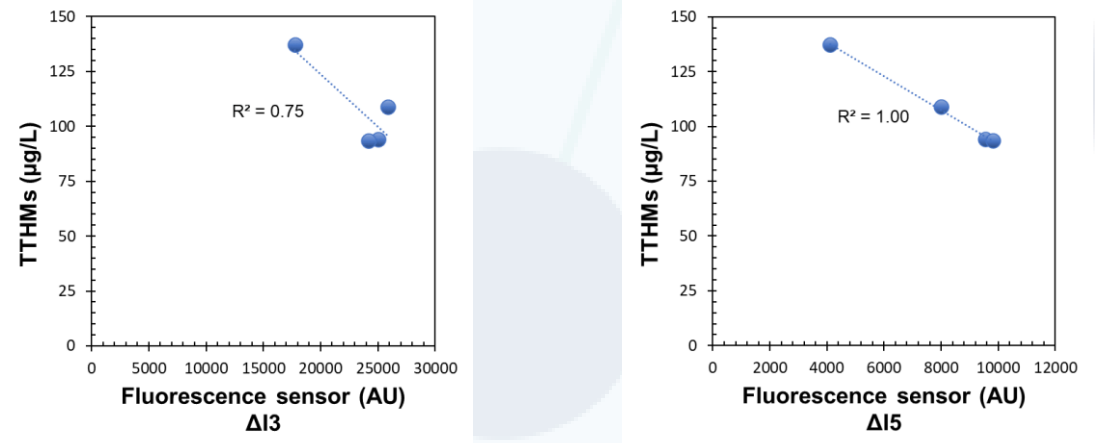
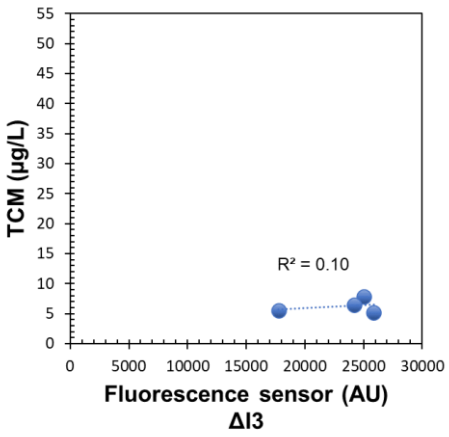
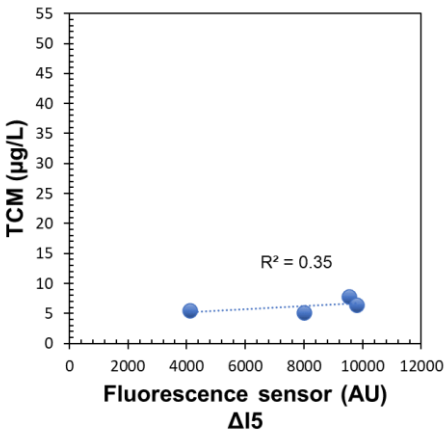
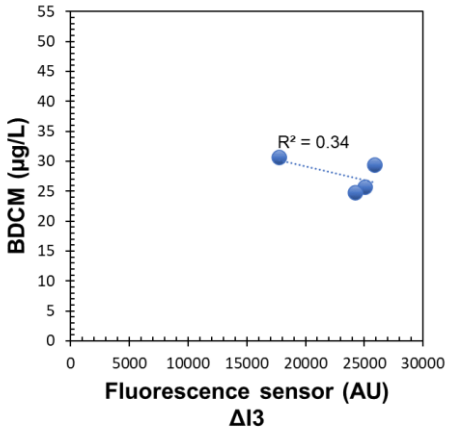


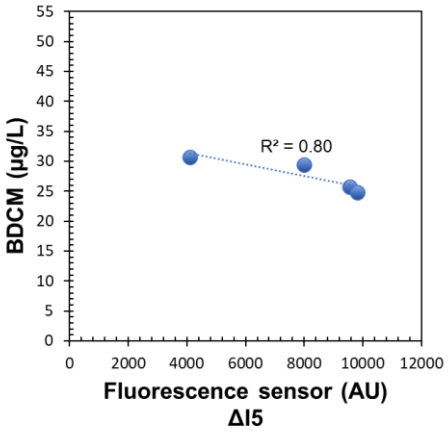
Figure 23. Linear correlations between fluorescence sensors I3 or I5 and trihalomethanes in FP tests performed in Cyprus water samples (March sampling campaign)

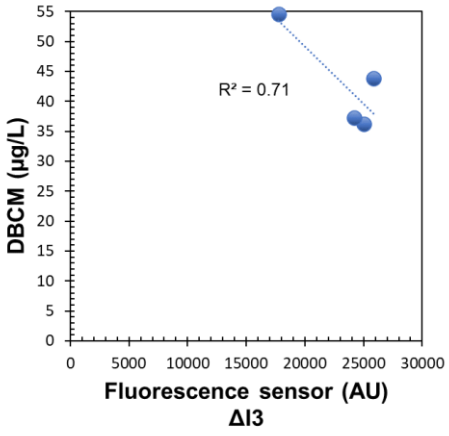


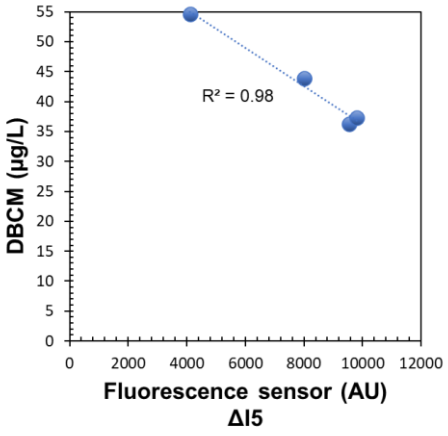

TCM (µg/L)
R² = 0.10
Fluorescence sensor (AU)
ΔI3


TCM (µg/L)
R² = 0.35
Fluorescence sensor (AU)
ΔI5


BDCM (µg/L)
R² = 0.34
Fluorescence sensor (AU)
ΔI3


BDCM (µg/L)
R² = 0.80
Fluorescence sensor (AU)
ΔI5


DBCM (µg/L)
R² = 0.71
Fluorescence sensor (AU)
ΔI3


DBCM (µg/L)
R² = 0.98
Fluorescence sensor (AU)
ΔI5

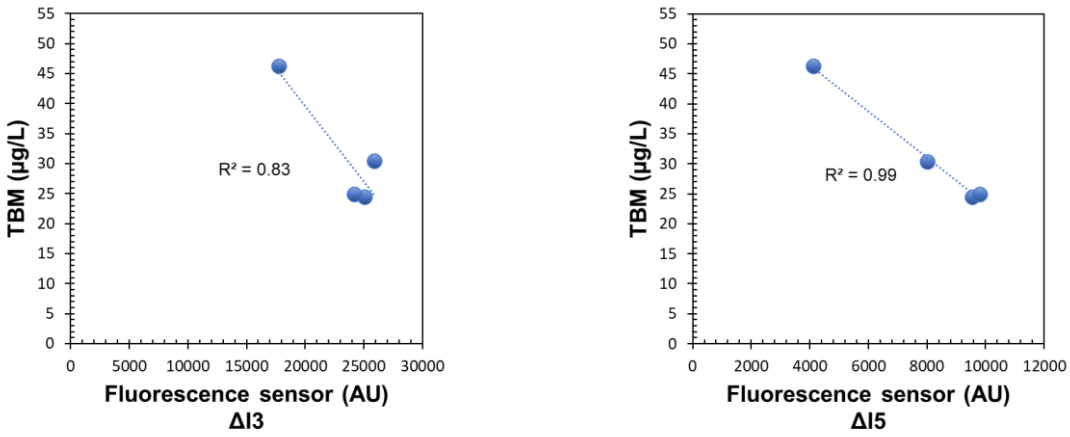


Figure 24. Linear correlations between differential fluorescence by sensors ΔI3 or ΔI5 and trihalomethanes in FP tests performed in Cyprus water samples (March sampling campaign)

5.2 DBPs concentrations

5.2.1 Correlation between DBPs and fluorescence signals from all the distribution system points at CS-1

Fluorescence sensors could be used to monitor the actual DBPs concentrations in the distribution systems. Therefore, samples from CS-1 were collected along the distribution network (from the DWTP outlet to the tap) and analysed for actual DBPs concentration and fluorescence by off-line sensors. Linear correlation models between fluorescence signals from the sensors and the corresponding actual DBPs concentrations were developed. Fluorescence signals were collected from both quenched (with sodium sulfite) and not quenched samples to evaluate the effect of quenching on the correlations. In particular, UCY carried out 3 sampling campaigns in February, March and April 2024, along the distribution network. The water was collected from the following points:

1. DWTP Outlet (sensor station)
2. Zone 2 inlet
3. Zone 2 outlet (sensor station)
4. DMA Inlet (sensor station)
5. Distribution Point 1
6. Distribution Point 2
7. Distribution Point 3 (sensor station)
8. Distribution Point 4

In Figure 25 the average (average values of the February and March sampling campaigns) concentrations of THMs found in the water samples from the distribution system of the CS-1 are reported. As expected, THMs concentrations increased significantly after the re-chlorination tank in “Zone 2”.

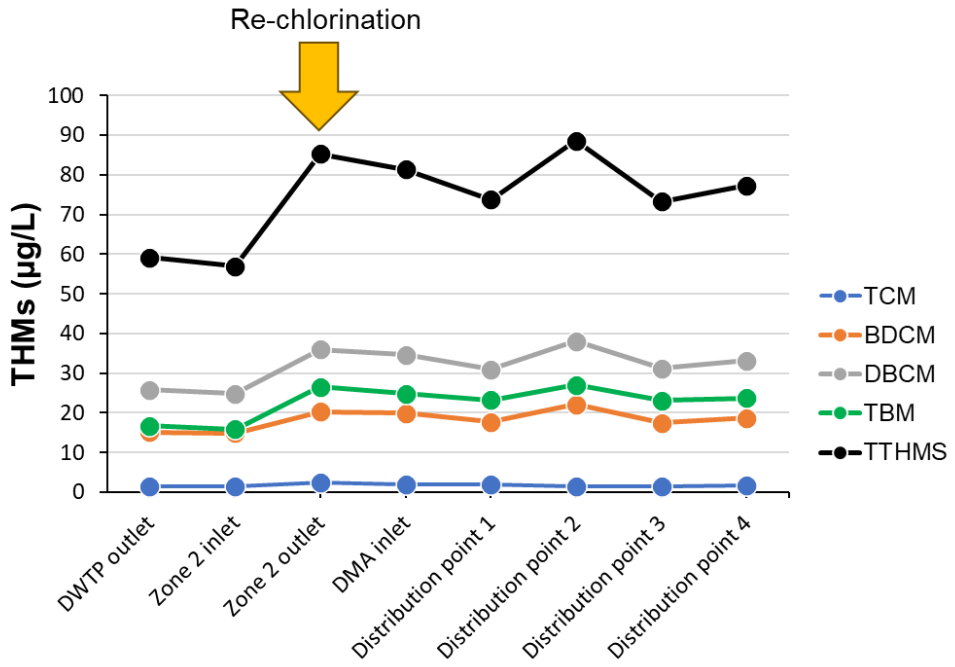


Figure 25. THMs levels in Cyprus samples (average values of February and March campaigns)

Linear correlation models between actual DBPs concentrations and fluorescence signals from sensor were developed.

Table 5 and Table 6 show the determination coefficients (R^2) for models with on-quenched and quenched samples, respectively. The data from all samples were collected during the February and March sampling campaigns.

Table 5. Determination coefficients (R^2) of linear correlation models between fluorescence by sensors and actual DBPs detected in non-quenched Cyprus water samples collected from all the distribution points (February and March sampling campaigns)

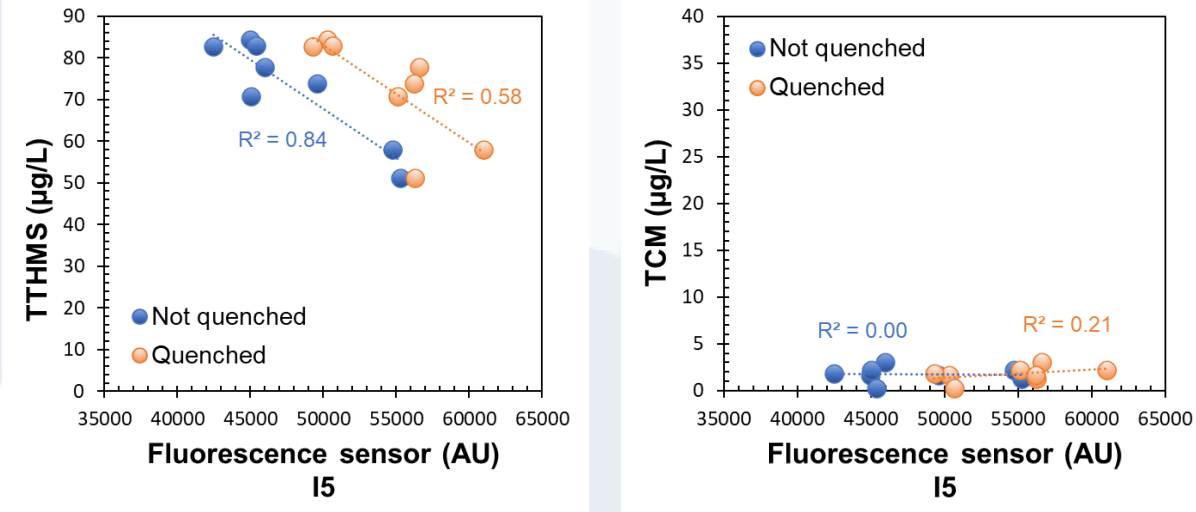
Sensor	TCM	BDCM	DBCM	TBM	TTHMs
	Sampling campaign: February				
I3	0.01	0.42	0.50	0.69	0.58
I5	0.00	**0.75**	**0.80**	**0.83**	**0.84**
	Sampling campaign: March				
I3	0.11	0.28	0.46	0.67	0.48
I5	0.23	0.46	0.55	0.59	0.55

Table 6. Determination coefficients (R^2) of linear correlation models between fluorescence by sensors and actual DBPs detected in quenched Cyprus water samples collected from all the distribution points (February and March sampling campaigns)

Sensor	TCM	BDCM	DBCM	TBM	TTHMs
	Sampling campaign: February				
I3	0.00	0.62	0.68	0.64	0.67
I5	0.21	0.50	0.64	0.62	0.58
	Sampling campaign: March				
I3	0.47	0.62	0.62	0.54	0.63
I5	0.32	0.50	0.50	0.42	0.50

Overall, some correlations exist between fluorescence signals from the sensors and THMs concentrations. The correlations obtained by the not quenched samples are better than those observed for quenched samples. This result could be ascribed to a negative effect of the quenching agent. However, the application of online sensors will not be influenced by any quenching agent. Notably, the correlations are better for data from the February campaign than for those from the March campaign. This could be a limitation due to the change of correlation with water quality that needs to be addressed during the online test that will be performed in WP3 activity.

As a representative example of correlation models for DBPs monitoring by fluorescence I5 sensor, regressions related to February campaign samples are shown in Figure 26.



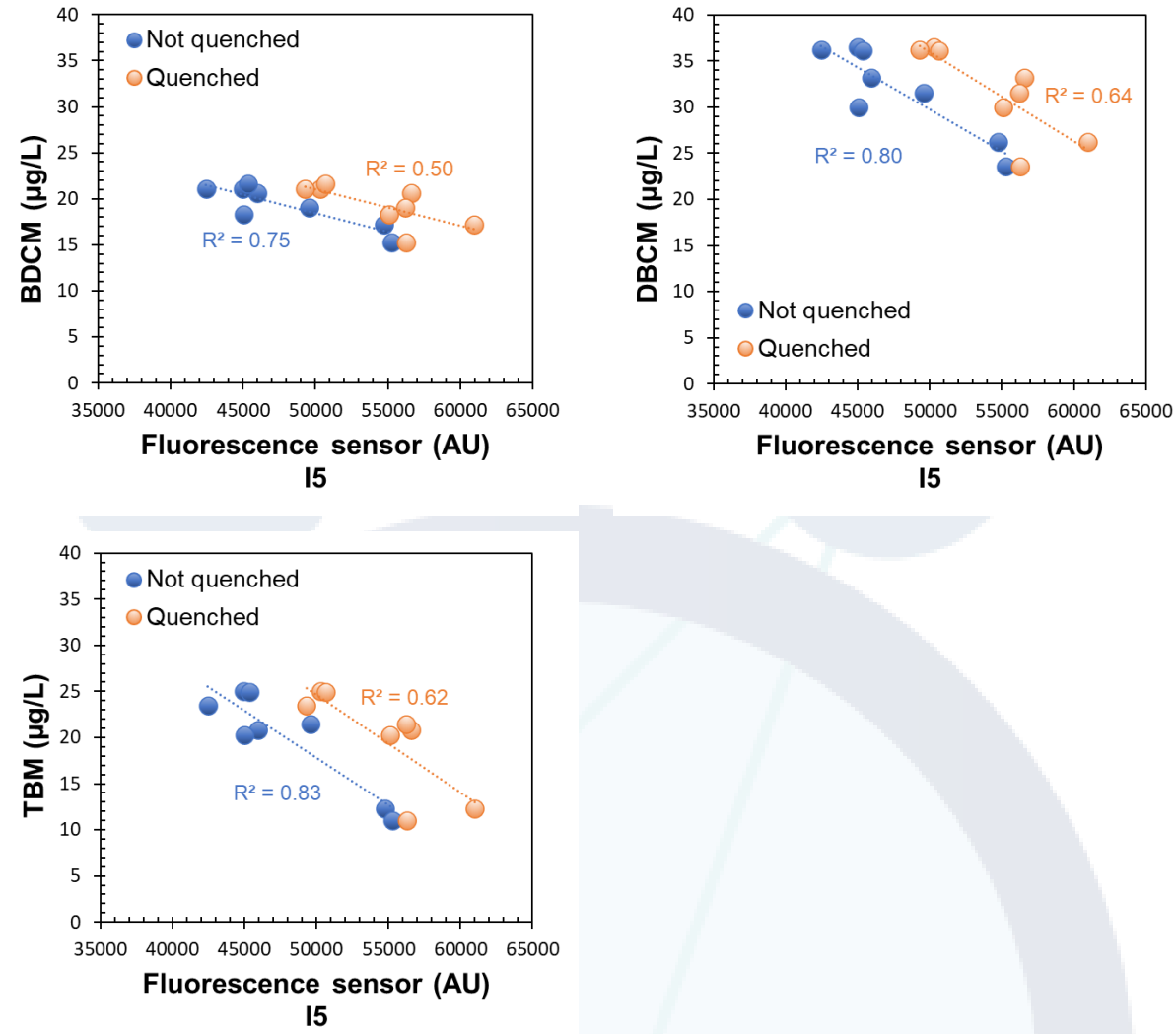


Figure 26. Linear correlations between actual DBPs concentrations and fluorescence signals sensor I5 detected in CS-1 quenched and non-quenched samples collected from all the points of the distribution system points (February sampling campaign)

5.2.2 Correlation between DBPs and fluorescence signals from the sensor stations within the distribution system at CS-1

In this section, a sub-dataset that includes only samples collected at sensor station points is used for developing some correlation models. The sensor station points are those points of the distribution system where sensor stations are already employed at the CS-1: DWTP outlet, Zone 2 outlet, DMA inlet and Distribution point 3.

Table 7 and Table 8 show the determination coefficient values (R^2) of linear correlations between fluorescence signals from sensors and the actual DBPs in either non-quenched or quenched samples (February and March sampling campaigns), respectively.

In this case, I3 showed strong correlations with actual THMs in quenched samples. I5 showed very good correlations for both quenched and non-quenched samples compared to the other samples. Figure 27 illustrates the linear correlations between I5 fluorescence

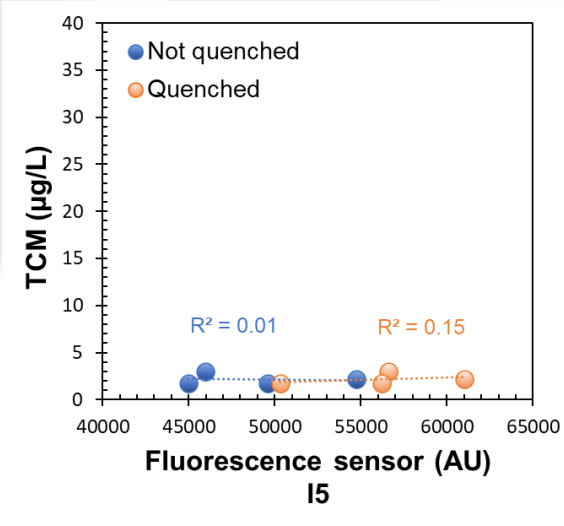
data and actual DBPs of quenched and non-quenched samples collected at the sensor stations (February sampling campaign).

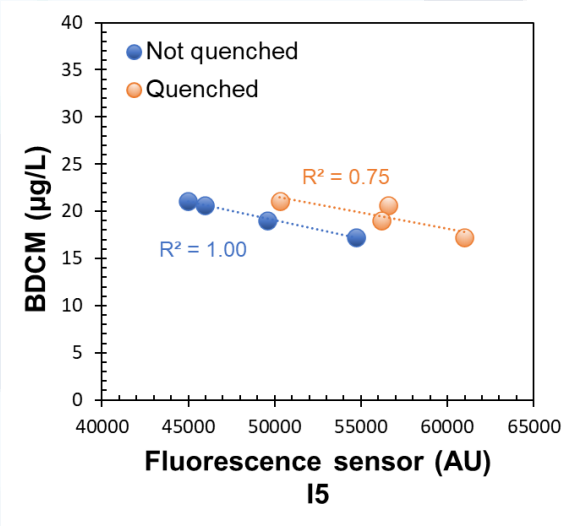
Table 7. R^2 coefficients of linear correlation models between fluorescence by sensors and actual DBPs detected in non-quenched Cyprus water samples collected at the sensor stations (February and March sampling campaigns)

Sensor	TCM	BDCM	DBCM	TBM	TTHMs
	Sampling campaign: February				
I3	0.34	0.19	0.33	0.57	0.58
I5	0.01	**1.00**	**0.94**	**0.85**	**0.96**
	Sampling campaign: March				
I3	0.25	0.50	**0.78**	**0.89**	**0.76**
I5	0.33	0.53	0.62	0.53	0.59

Table 8. R2 coefficients of linear correlation models between fluorescence by sensors and actual DBPs detected in quenched Cyprus water samples collected at the sensor stations (February and March sampling campaigns)

Sensor	TCM	BDCM	DBCM	TBM	TTHMs
	Sampling campaign: February				
I3	0.00	**0.96**	**0.93**	**0.75**	**0.89**
I5	0.15	**0.75**	**0.91**	**0.87**	**0.86**
	Sampling campaign: March				
I3	0.64	**0.75**	0.67	0.46	0.65
I5	0.45	0.57	0.50	0.33	0.48





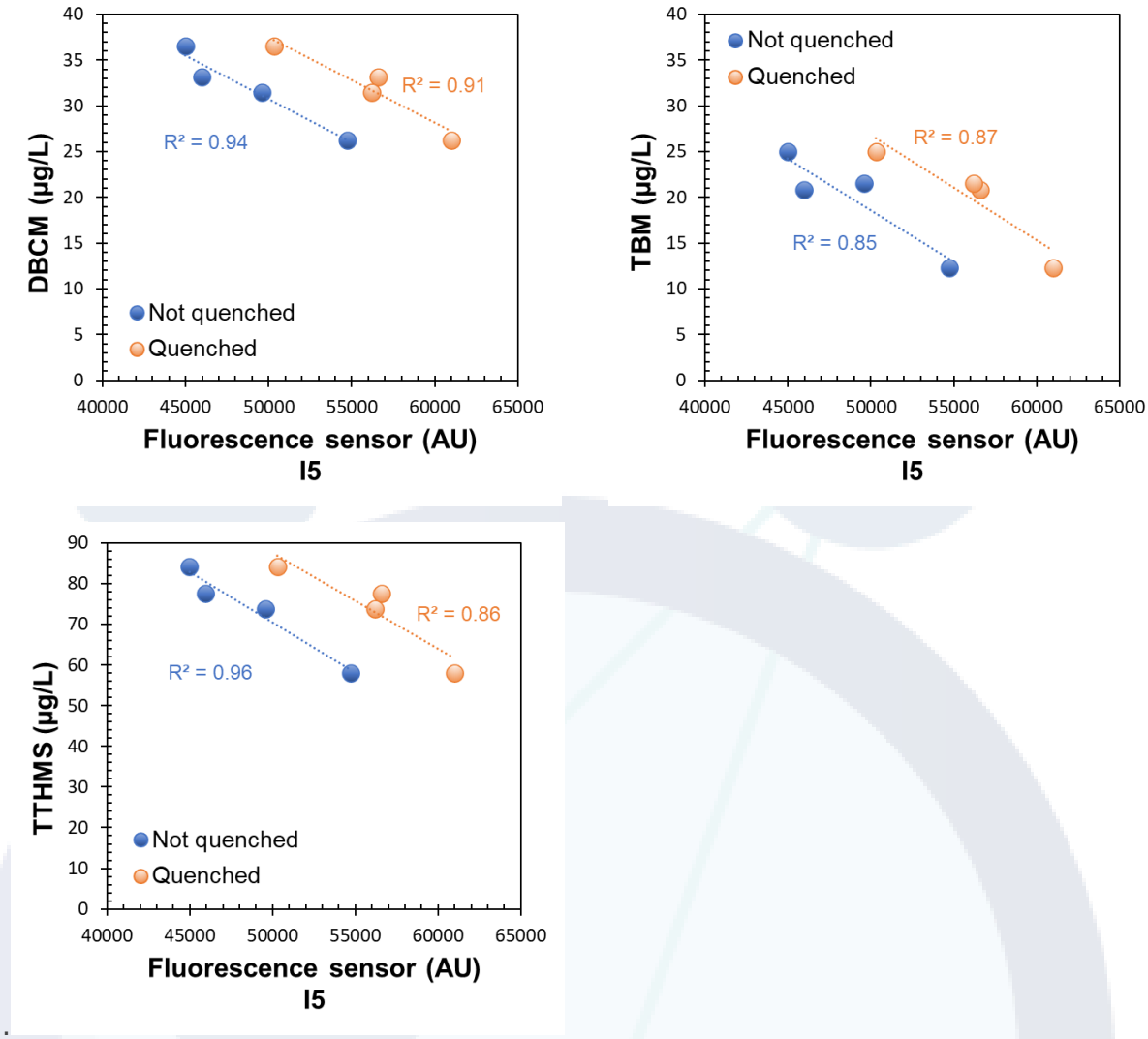


Figure 27. Linear correlations between actual DBPs concentrations and fluorescence by sensor I5 detected in Cyprus quenched and non-quenched samples collected at the sensor stations (February sampling campaign)

In conclusion, monitoring of actual DBPs via fluorescence sensors is promising. It has been noted that the location of the sensors is crucial for developing robust predictive models. Good results were obtained for the dataset of samples that considers the points of the sensor stations. Furthermore, the I5 sensor appears the most suitable for monitoring DBPs, having shown strong correlations for quenched and non-quenched samples of the CS-1.

6.0 FLUORESCENCE TOOL CHARACTERISTICS

The fluorescence tool developed in this project to predict/monitor DBPs and DBPs precursors in chlorinated water is made by a customized Photometric Transmitter (PT) connected with a fluorescence probe through a fiber optic cable. The fluorescence tool provides fluorescence signals at a selected excitation/emission wavelength pair ($\lambda_{ex}/\lambda_{em}$) that can be monitored via software.

The PT unit is equipped with both analogic and digital forms of communication, which allows communication with any PLC. The analogic is a 4-20mA output, while the digital uses a modbus protocol RS485.

Figure 28 shows a picture of both the Photometric Transmitter (PT) and the probe of the customized fluorescence tool, while Figure 29 shows a detail of an online connection of the fluorescence probe.

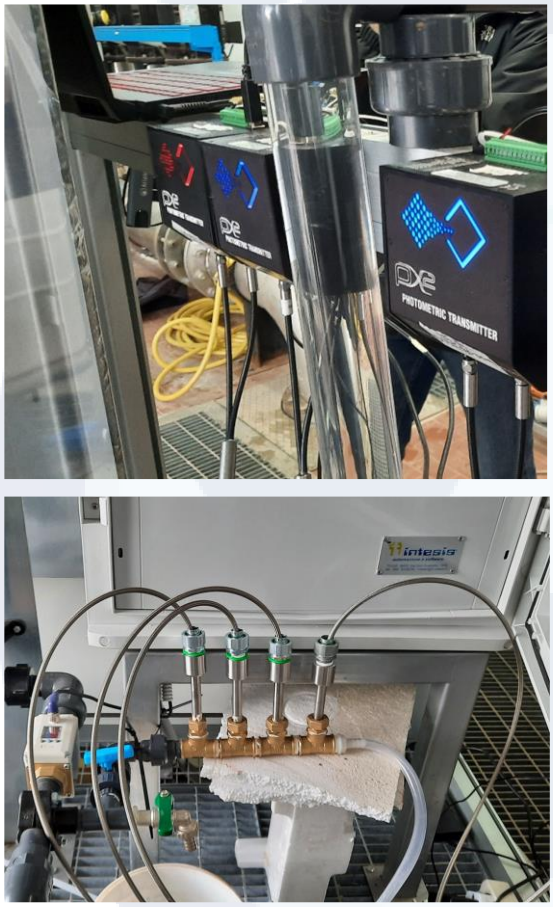


Figure 28. Picture of the Photometric Transmitter (PT) (top) and probe (bottom) of the customized fluorescence tool



Figure 29. Detail of an online connection of the fluorescence probe

7.0 CONCLUSIONS

From the results shown in this report, the following conclusion can be drawn:

- The prototype fluorescence tool developed in this project to predict/monitor DBPs and DBPs precursors in chlorinated water is made by a customized Photometric Transmitter (PT) connected with a fluorescence probe through a fiber optic cable;
- The fluorescence tool provides fluorescence signals at a selected excitation/emission wavelength pair ($\lambda_{ex}/\lambda_{em}$) that can be monitored via dedicated software;
- The first step of the prototype development required the study of the literature and prior data on EEM of different water quality from the UCT team;
- The second step consisted of the study of EEMs of waters from intoDBP CSs to validate the effectiveness of the selected fluorescence ex/em pairs in tracking DBPs and their precursors;
- The excitation/emission pairs selected based on prior publications and data obtained from the intoDBP project are two: I3(ex257,em440) and I5 (ex325,em448);
- Two prototype fluorescence tools were developed and tested. One is equipped with the I3(ex257,em440) and one with the I5 (ex325,em448);
- The PT unit is equipped with both analogic and digital forms of communication, which allows communication with any PLC. The analogic is a 4-20mA output, while the digital uses a modbus protocol RS485.
- The third step of the prototype fluorescence tool development required the calibration of the sensors by using different waters, which were diluted to autotune the sensor;
- The fourth step of the prototype fluorescence tool development was the validation of the sensor signals. For this purpose, the signals obtained from the sensor were correlated with the corresponding values (ex/em fluorescence data extracted from the EEM) obtained by the laboratory spectrofluorometer; this correlation was made by using different water qualities, including waters collected in the Catania area and at the CSs. In particular, some water samples were collected with and without the addition of a quenching agent to reduce the chlorine. The observed correlations were always strong, regardless of the presence of the quenching agent. When the fluorescence sensors were calibrated on the same water, high correlations were found by comparing data from all the case studies (Madrid, Barcelona, Cyprus): $R^2 = 0.94$ and $R^2 = 0.98$ for I3 and I5 sensors, respectively. This fact underlines the importance of using the same calibration for comparing data from different waters;
- The final step of the prototype fluorescence tool development was the validation of the sensor signals to predict DBPFP or DBPs concentrations in the waters from the CSs. The results highlight that both I3 and I5 were effective in tracking the reactivity of NOM in DBPs formation (DBPFP). The differential I3 and I5 values were also correlated and the correlations with DBPFP were comparable to those observed for I3 and I5. Finally, the values of the I5 index were well correlated with the THMs concentrations measured in the Limassol distribution systems. In particular, better correlations were found for the not quenched samples. It is noteworthy to mention that the correlations between I5 and THMs were very good for a subset of data

belonging to the stations where other sensors are already installed. This is an important result because the fluorescence tool will be installed in those stations.



8.0 REFERENCES

APHA, 1998. Standard Methods for the Examination of Water and Wastewater. American Public Health Association.

Beauchamp, N., Laflamme, O., Simard, S., Dorea, C., Pelletier, G., Bouchard, C., Rodriguez, M., 2018. Relationships between DBP concentrations and differential UV absorbance in full-scale conditions. Water Res. 131, 110–121. https://doi.org/10.1016/j.watres.2017.12.031

Bridgeman, J., Bieroza, M., Baker, A., 2011. The application of fluorescence spectroscopy to organic matter characterisation in drinking water treatment. Rev. Environ. Sci. Biotechnol. 10, 277–290. https://doi.org/10.1007/s11157-011-9243-x

Bugden, J.B.C., Yeung, C.W., Kepkay, P.E., Lee, K., 2008. Application of ultraviolet fluorometry and excitation–emission matrix spectroscopy (EEMS) to fingerprint oil and chemically dispersed oil in seawater. Mar. Pollut. Bull. 56, 677–685. https://doi.org/10.1016/j.marpolbul.2007.12.022

Chen, W., Westerhoff, P., Leenheer, J.A., Booksh, K., 2003. Fluorescence Excitation−Emission Matrix Regional Integration to Quantify Spectra for Dissolved Organic Matter. Environ. Sci. Technol. 37, 5701–5710. https://doi.org/10.1021/es034354c

Chin, Y.-Ping., Aiken, George., O'Loughlin, Edward., 1994. Molecular Weight, Polydispersity, and Spectroscopic Properties of Aquatic Humic Substances. Environ. Sci. Technol. 28, 1853–1858. https://doi.org/10.1021/es00060a015

Croue, J.-P., Korshin, G.V., Benjamin, M.M., 2000. Characterization of Natural Organic Matter in Drinking Water. American Water Works Association.

Dejaeger, K., Criquet, J., Vanoppen, M., Vignal, C., Billon, G., Cornelissen, E.R., 2022. Identification of disinfection by-product precursors by natural organic matter fractionation: a review. Environ. Chem. Lett. 20, 3861–3882. https://doi.org/10.1007/s10311-022-01478-x

Deng, Y., Mo, S., Korshin, G.V., Yan, M., 2024. A universal model to predict yields of THMs and HAAs based on UV–Visible absorption spectra. Water Res. 254, 121367. https://doi.org/10.1016/j.watres.2024.121367

Fabbricino, M., Korshin, G.V., 2005. Formation of disinfection by-products and applicability of differential absorbance spectroscopy to monitor halogenation in chlorinated coastal and deep ocean seawater. Desalination 176, 57–69. https://doi.org/10.1016/j.desal.2004.10.026

Hong, H.C., Huang, F.Q., Wang, F.Y., Ding, L.X., Lin, H.J., Liang, Y., 2013. Properties of sediment NOM collected from a drinking water reservoir in South China, and its association with THMs and HAAs formation. J. Hydrol. 476, 274–279. https://doi.org/10.1016/j.jhydrol.2012.10.040

Hu, J., Xiao, R., Zhang, R., Wu, Z., Jiang, F., Ye, C., Qu, R., Chu, W., 2024. Application of EEM fluorescence spectroscopy for characterizing organic DBP precursors in different water sources: a review. AQUA — Water Infrastruct. Ecosyst. Soc. 73, 464–486. https://doi.org/10.2166/aqua.2024.255

Hua, L.-C., Chao, S.-J., Huang, K., Huang, C., 2020. Characteristics of low and high SUVA precursors: Relationships among molecular weight, fluorescence, and chemical composition with DBP formation. Sci. Total Environ. 727, 138638. https://doi.org/10.1016/j.scitotenv.2020.138638

Hudson, N., Baker, A., Reynolds, D., 2007. Fluorescence analysis of dissolved organic matter in natural, waste and polluted waters—a review. River Res. Appl. 23, 631–649. https://doi.org/10.1002/rra.1005

Jing, Z.-B., Wang, W.-L., Nong, Y.-J., Zhu, P., Lu, Y., Wu, Q.-Y., 2022. Fluorescence analysis for water characterization: measurement processes, influencing factors, and data analysis. J. Water Reuse Desalination jwrd2022065. https://doi.org/10.2166/wrd.2022.065

Karanfil, T., Schlautman, M.A., Erdogan, I., 2002. Survey of DOC and UV measurement practices with implications for SUVA determination. J. AWWA 94, 68–80. https://doi.org/10.1002/j.1551-8833.2002.tb10250.x

Kitis, M., Karanfil, T., Kilduff, J.E., Wigton, A., 2001. The reactivity of natural organic matter to disinfection by-products formation and its relation to specific ultraviolet absorbance. Water Sci. Technol. 43, 9–16. https://doi.org/10.2166/wst.2001.0067

Kitis, M., Karanfil, T., Wigton, A., Kilduff, J.E., 2002. Probing reactivity of dissolved organic matter for disinfection by-product formation using XAD-8 resin adsorption and ultrafiltration fractionation. Water Res. 36, 3834–3848. https://doi.org/10.1016/S0043-1354(02)00094-5

Korshin, G.V., Li, C.-W., Benjamin, M.M., 1996. Use of UV Spectroscopy To Study Chlorination of Natural Organic Matter, in: Water Disinfection and Natural Organic Matter, ACS Symposium Series. American Chemical Society, pp. 182–195. https://doi.org/10.1021/bk-1996-0649.ch012

Korshin, G.V., Sgroi, M., Ratnaweera, H., 2018. Spectroscopic surrogates for real time monitoring of water quality in wastewater treatment and water reuse. Curr. Opin. Environ. Sci. Health 2, 12–19. https://doi.org/10.1016/j.coesh.2017.11.003

Li, L., Wang, Y., Zhang, W., Yu, S., Wang, X., Gao, N., 2020. New advances in fluorescence excitation-emission matrix spectroscopy for the characterization of dissolved organic matter in drinking water treatment: A review. Chem. Eng. J. 381, 122676. https://doi.org/10.1016/j.cej.2019.122676

McKnight, D.M., Boyer, E.W., Westerhoff, P.K., Doran, P.T., Kulbe, T., Andersen, D.T., 2001. Spectrofluorometric characterization of dissolved organic matter for indication of precursor organic material and aromaticity. Limnol. Oceanogr. 46, 38–48. https://doi.org/10.4319/lo.2001.46.1.0038

Murphy, K.R., Butler, K.D., Spencer, R.G.M., Stedmon, C.A., Boehme, J.R., Aiken, G.R., 2010. Measurement of Dissolved Organic Matter Fluorescence in Aquatic Environments: An Interlaboratory Comparison. Environ. Sci. Technol. 44, 9405–9412. https://doi.org/10.1021/es102362t

Nguyen, H.V.-M., Tak, S., Hur, J., Shin, H.-S., 2023. Fluorescence spectroscopy in the detection and management of disinfection by-product precursors in drinking water treatment processes: A review. Chemosphere 343, 140269. https://doi.org/10.1016/j.chemosphere.2023.140269

Peuravuori, J., Monteiro, A., Eglite, L., Pihlaja, K., 2005. Comparative study for separation of aquatic humic-type organic constituents by DAX-8, PVP and DEAE sorbing solids and tangential ultrafiltration: elemental composition, size-exclusion chromatography, UV–vis and FT-IR. Talanta, Evaluation/Validation of Novel Biosensors in Real Environmental and Food Samples 65, 408–422. https://doi.org/10.1016/j.talanta.2004.06.042

Peuravuori, J., Pihlaja, K., 2004. Preliminary Study of Lake Dissolved Organic Matter in Light of Nanoscale Supramolecular Assembly. Environ. Sci. Technol. 38, 5958–5967. https://doi.org/10.1021/es040041l

Peuravuori, J., Pihlaja, K., 1997. Molecular size distribution and spectroscopic properties of aquatic humic substances. Anal. Chim. Acta 337, 133–149. https://doi.org/10.1016/S0003-2670(96)00412-6

Richardson, S.D., Thruston, A.D., Rav-Acha, C., Groisman, L., Popilevsky, I., Juraev, O., Glezer, V., McKague, A.B., Plewa, M.J., Wagner, E.D., 2003. Tribromopyrrole, Brominated Acids,

and Other Disinfection Byproducts Produced by Disinfection of Drinking Water Rich in Bromide. Environ. Sci. Technol. 37, 3782–3793. https://doi.org/10.1021/es030339w

Roccaro, P., Chang, H.-S., Vagliasindi, F.G.A., Korshin, G.V., 2008. Differential absorbance study of effects of temperature on chlorine consumption and formation of disinfection by-products in chlorinated water. Water Res. 42, 1879–1888. https://doi.org/10.1016/j.watres.2007.11.013

Roccaro, P., Vagliasindi, F.G.A., 2009. Differential vs. absolute UV absorbance approaches in studying NOM reactivity in DBPs formation: Comparison and applicability. Water Res. 43, 744–750. https://doi.org/10.1016/j.watres.2008.11.007

Roccaro, P., Vagliasindi, F.G.A., Korshin, G.V., 2009. Changes in NOM Fluorescence Caused by Chlorination and their Associations with Disinfection by-Products Formation. Environ. Sci. Technol. 43, 724–729. https://doi.org/10.1021/es801939f

Sgroi, M., Gagliano, E., Vagliasindi, F.G.A., Roccaro, P., 2020a. Inner filter effect, suspended solids and nitrite/nitrate interferences in fluorescence measurements of wastewater organic matter. Sci. Total Environ. 711. https://doi.org/10.1016/j.scitotenv.2019.134663

Sgroi, M., Gagliano, E., Vagliasindi, F.G.A., Roccaro, P., 2020b. Absorbance and EEM fluorescence of wastewater: Effects of filters, storage conditions, and chlorination. Chemosphere 243. https://doi.org/10.1016/J.CHEMOSPHERE.2019.125292

Sgroi, M., Pelissari, C., Roccaro, P., Sezerino, P.H., García, J., Vagliasindi, F.G.A., Ávila, C., 2018. Removal of organic carbon, nitrogen, emerging contaminants and fluorescing organic matter in different constructed wetland configurations. Chem. Eng. J. 332, 619–627. https://doi.org/10.1016/J.CEJ.2017.09.122

Sgroi, M., Roccaro, P., Korshin, G.V., Greco, V., Sciuto, S., Anumol, T., Snyder, S.A., Vagliasindi, F.G.A., 2017a. Use of fluorescence EEM to monitor the removal of emerging contaminants in full scale wastewater treatment plants. J. Hazard. Mater. 323, 367–376. https://doi.org/10.1016/j.jhazmat.2016.05.035

Sgroi, M., Roccaro, P., Korshin, G.V., Greco, V., Sciuto, S., Anumol, T., Snyder, S.A., Vagliasindi, F.G.A., 2017b. Use of fluorescence EEM to monitor the removal of emerging contaminants in full scale wastewater treatment plants. J. Hazard. Mater. 323, 367–376. https://doi.org/10.1016/j.jhazmat.2016.05.035

Summers, R.S., Hooper, S.M., Shukairy, H.M., Solarik, G., Owen, D., 1996. Assessing DBP yield: uniform formation conditions. J. AWWA 88, 80–93. https://doi.org/10.1002/j.1551-8833.1996.tb06573.x

Traina, S.J., Novak, J., Smeck, N.E., 1990. An Ultraviolet Absorbance Method of Estimating the Percent Aromatic Carbon Content of Humic Acids. J. Environ. Qual. 19, 151–153. https://doi.org/10.2134/jeq1990.00472425001900010023x

Weishaar, J.L., Aiken, G.R., Bergamaschi, B.A., Fram, M.S., Fujii, R., Mopper, K., 2003. Evaluation of Specific Ultraviolet Absorbance as an Indicator of the Chemical Composition and Reactivity of Dissolved Organic Carbon. Environ. Sci. Technol. 37, 4702–4708. https://doi.org/10.1021/es030360x

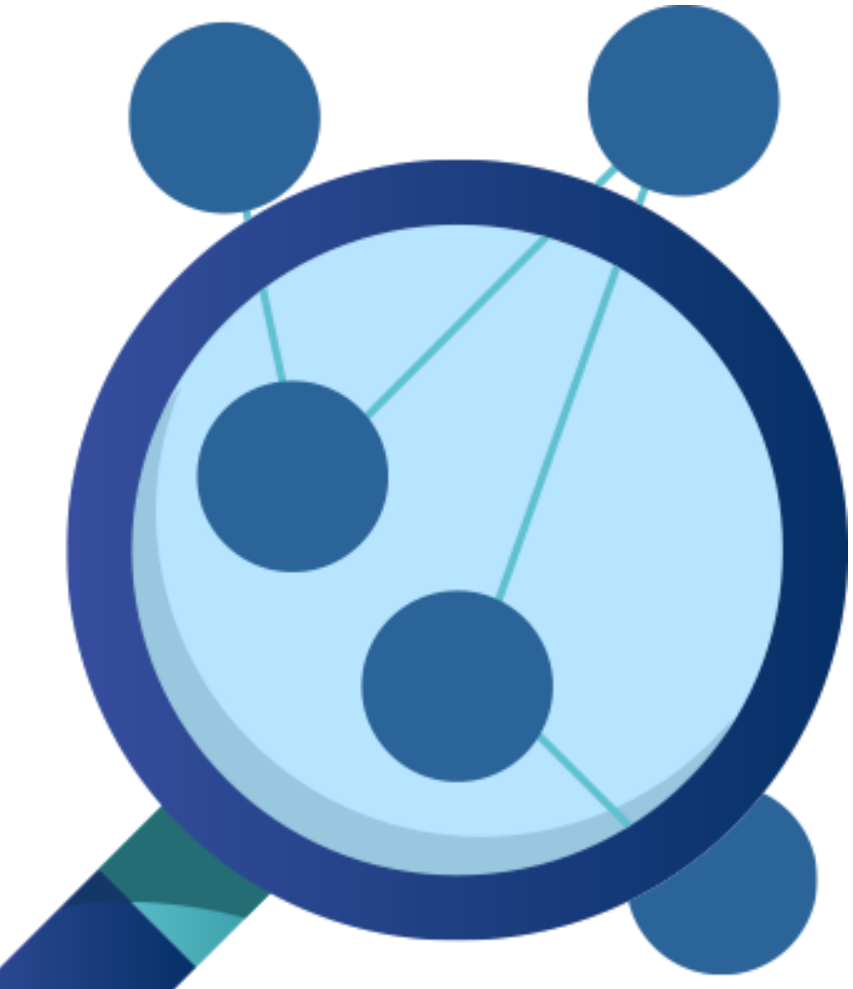
Wu, F.C., Kothawala, D.N., Evans, R.D., Dillon, P.J., Cai, Y.R., 2007. Relationships between DOC concentration, molecular size and fluorescence properties of DOM in a stream. Appl. Geochem. 22, 1659–1667. https://doi.org/10.1016/j.apgeochem.2007.03.024

Wu, W.W., Chadik, P.A., Davis, W.M., Delfino, J.J., Powell, D.H., 2000. The Effect of Structural Characteristics of Humic Substances on Disinfection By-Product Formation in Chlorination, in: Natural Organic Matter and Disinfection By-Products, ACS Symposium Series. American Chemical Society, pp. 109–121. https://doi.org/10.1021/bk-2000-0761.ch008

Yang, X., Shang, C., Lee, W., Westerhoff, P., Fan, C., 2008. Correlations between organic matter properties and DBP formation during chloramination. Water Res. 42, 2329–2339. https://doi.org/10.1016/j.watres.2007.12.021

Zhang, C., Chen, B., Korshin, G.V., Kuznetsov, A.M., Roccaro, P., Yan, M., Ni, J., 2020. Comparison of the yields of mono-, Di- and tri-chlorinated HAAs and THMs in chlorination and chloramination based on experimental and quantum-chemical data. Water Res. 169, 115100. https://doi.org/10.1016/j.watres.2019.115100

Zhang, C., Roccaro, P., Yan, M., Korshin, G.V., 2021. Interpretation of the formation of unstable halogen-containing disinfection by-products based on the differential absorbance spectroscopy approach. Chemosphere 268, 129241. https://doi.org/10.1016/j.chemosphere.2020.129241



intoDBP

Funded by
the European Union